Assessing Earth system responses in mitigation scenarios with activity-driven simulation of carbon dioxide removal

Jörg Schwinger[1], Leon Merfort[2], Nico Bauer[2], Raffaele Bernardello[3], Momme Butenschön[4], Timothée Bourgeois[1], Matthew J. Gidden[5,6], Shraddha Gupta[7], Hanna Lee[8], Nadine Mengis[9], Yiannis Moustakis[7,10], Helene Muri[8,11], Lars Nieradzik[12], Daniele Peano[4], Julia Pongratz[7], Pascal Sauer[2], Etienne Tourigny[3], David Wårlind[12]

[1] NORCE Climate & Environment, Bjerknes Centre for Climate Research, Bergen, Norway
[2] Potsdam Institute for Climate Impact Research, Potsdam, Member of the Leibniz Association, Germany
[3] Barcelona Supercomputing Center, Barcelona, Spain
[4] CMCC Foundation - Euro-Mediterranean Center on Climate Change, Italy
[5] International Institute for Applied Systems Analysis, Laxenburg, Austria
[6] Center for Global Sustainability, University of Maryland, College Park, USA
[7] Ludwig-Maximilians-Universität München, Munich, Germany
[8] Norwegian University of Science and Technology, Trondheim, Norway
[9] GEOMAR Helmholtz Centre for Ocean Research Kiel, Kiel, Germany
[10] Imperial College London, London, United Kingdom
[11] NILU, Kjeller, Norway
[12] Department of Earth and Environmental Sciences, Lund University, Lund, Sweden

Correspondence to: Jörg Schwinger (jorg.schwinger0@gmail.com)

Abstract. Assessing Earth system responses arising from carbon dioxide removal (CDR) requires developing and simulating pairs of scenarios - a mitigation scenario with deployment of CDR and a corresponding no-CDR baseline. The latter describes a world where no CDR is deployed, such that net carbon emissions are higher and a given temperature target may be missed. While over the past years a rich literature on deep mitigation scenarios with CDR has been emerging, no-CDR baselines have mostly been explored in stylized Earth system model (ESM) experiments. In such simulations, a no-CDR baseline simply assumes that CDR is “switched off”, while socio-economic constraints are not considered. However, the deployment of CDR in mitigation scenarios, created by integrated assessment models (IAMs), is embedded in a consistent socio-economic description of plausible futures, and disallowing CDR may affect climate drivers due to changes in the energy system and in land-use dynamics. Particularly, when moving towards an activity-driven representation of CDR in emission-driven ESMs, where the activity that draws down CO_2 from the atmosphere is explicitly modelled, the creation of no-CDR baselines comes with challenges and trade-offs. Here, we conceptualize a framework for emission-driven ESM simulations of IAM scenarios that allows us to determine carbon-cycle feedbacks and biogeophysical effects of CDR

deployment using no-CDR baselines. We show that different options exist for the creation of no-CDR baselines, which offer different insights and have their specific advantages and limitations. We also demonstrate that internal variability of the climate system inherently limits our ability to detect the small signals related to CDR deployment and its feedbacks. Hence, unless a sufficiently large initial conditions ensemble is employed, stylized modelling approaches may remain preferable for some applications, e.g., the quantification of regional biogeophysical effects of CDR deployment. Both, the efficiency of CDR as well as related carbon-cycle feedbacks and biogeophysical effects are expected to be scenario- and model-dependent. Our simulation design of concentration- and emission-driven no-CDR baselines, together with an improved representation of CDR in the IAM - ESM modelling chain, opens an avenue towards estimating CDR efficiencies and their uncertainties under various future scenarios in upcoming model intercomparison activities.

1. Introduction

Since the enactment of climate change mitigation policies has been delayed over the past decades, CDR is now a necessary, although not sufficient, mitigation option to keep global mean temperature below the 1.5°C limit established by the Paris Agreement in 2015. Achieving net-zero emissions requires CDR to compensate for residual emissions that are too expensive or technically impossible to mitigate (Buck et al., 2023; Merfort et al., 2023; Schenuit et al., 2023). In addition, fair burden sharing schemes might require high-income countries to deploy CDR (Bauer et al., 2020b). If stringent mitigation is further delayed, large-scale CDR might be the only option to return the Earth system to a less dangerous state after a temperature overshoot. There are many uncertainties surrounding CDR as issues related to socio-economic, technological, ecological, legal, governance, and ethical constraints are under discussion and require timely scientific investigation.

From an Earth system perspective, key uncertainties associated with a large-scale deployment of CDR are related to carbon-cycle feedbacks (e.g., Keller et al., 2014, 2018b; Oschlies, 2009; Schwinger et al., 2022) and biogeophysical effects and feedbacks (Amali et al., 2025; Boysen et al., 2014; Brovkin et al., 2013; De Noblet-Ducoudré et al., 2012; Zickfeld et al., 2023). Such feedbacks critically influence the overall effectiveness and costs of CDR, and a solid knowledge base is needed to inform mitigation policies and regulatory frameworks. The overarching key questions that need to be addressed urgently include: How much carbon is captured and stored by a specific CDR method and how is this efficiency altered by carbon cycle feedbacks, particularly if CDR is deployed at large-scale relying on a portfolio of methods? What is the contribution of CDR-related changes in land surface properties to alterations of the surface climate (biogeophysical effects)? How does the efficiency vary spatially and over time as climate change unfolds for a given future scenario? What is the response of fast and slow components of the Earth system to CDR, that is, can CDR restore a previous climate state after an overshoot and what are the timescales? At what level of certainty can Earth system responses and feedbacks be identified?

The best available tools to address such questions are fully coupled Earth system models (ESMs). ESMs have been used to investigate many aspects of large-scale CDR deployment including Earth system impacts, carbon-cycle feedbacks, and biogeophysical effects in a multitude of studies (e.g., Boucher et al., 2012; Egerer et al., 2024; Keller et al., 2018b; Li et al., 2023; Loughran et al., 2023; Melnikova et al., 2022, 2023; Moustakis et al., 2024; Schwinger et al., 2022; Sonntag et al., 2018; Tokarska and Zickfeld, 2015; Wang et al., 2021). However, the CDR deployment in such studies typically lacks the socio-economic consistency of mitigation scenarios generated by integrated assessment models (IAMs), which include CDR deployment based on estimates of their cost, energy demand, and land-use footprint as well as policy assumptions, thereby delivering a consistent picture of the role of CDR under various assumptions and constraints. A robust assessment of CDR needs to consider both the Earth system perspective and socio-economic constraints, and we therefore need to ensure a consistent representation of CDR across the IAM – ESM modelling chain.

IAMs are now being upgraded to include a larger portfolio of CDR methods (Bergero et al., 2024; Fuhrman et al., 2023; Gidden et al., 2023; Kowalczyk et al., 2024; Strefler et al., 2021, 2025), and in parallel ESMs expand their capacities to simulate in detail various land- and ocean-based CDR methods (e.g., Egerer et al., 2024; Melnikova et al., 2022; Moustakis et al., 2025; Schwinger et al., 2024; Wu et al., 2023). Importantly, fully coupled ESMs can represent many CDR methods by the activity that leads to the removal of CO_2 from the atmosphere together with possible other effects on the Earth system. For example, growing bioenergy crops, harvesting the biomass, and storing a part of the biomass carbon underground would model the process of bioenergy production with carbon capture and storage (BECCS). Modelling this activity explicitly in an ESM is in contrast to using the IAM estimate of the carbon removal and prescribing this negative emission flux in the ESM (prescribed CDR). *Activity-driven* simulation of CDR (Sanderson et al., 2024; see Sect. 2) harnesses the full potential of ESMs and has the advantage that climate change effects on the efficiency of CDR as well as biogeophysical effects are explicitly modelled. For terrestrial CDR methods, these include changes in plant physiological processes (e.g. stomatal conductance, water-use efficiency, heat/drought stress), biogeochemical feedbacks affecting carbon cycling, and biogeophysical effects such as changes in surface albedo and roughness. For marine CDR methods, the efficiency depends on ocean circulation and mixing and the various carbon pumps of the ocean (Hauck et al., 2016; Moustakis et al., 2025; Oschlies, 2009; Schwinger et al., 2024), which are explicitly modelled in ESMs but need to be parameterized in IAMs.

Achieving a robust assessment of CDR in deep mitigation pathways requires a fundamental shift in how IAM-derived scenarios are incorporated into ESMs. Although IAM and ESM modelling approaches have been aligned in large model intercomparison projects such as the ScenarioMIP (O'Neill et al., 2016; Van Vuuren et al., 2025), the representation of CDR has been quite limited so far. This was on the one hand due to the reliance on concentration-driven simulations in past phases of the Coupled Model Intercomparison Project (e.g., CMIP6; Eyring et al., 2016), where atmospheric CO_2 levels are prescribed to the ESMs rather than dynamically simulated from emissions. This approach restricts the ability of ESMs to fully capture Earth system feedbacks of CDR. On the other hand, CDR has not been simulated in an activity-driven way in any CMIP scenario so far (except for afforestation/reforestation (A/R), which is always activity-driven in ESMs, see section 2.2). While many mitigation scenarios from CMIP6 ScenarioMIP included A/R and BECCS, the underlying land-use changes and their resulting CO_2-fluxes were treated separately. In particular, the land-use forcings were provided explicitly (Hurtt et al. 2020), whereas the resulting carbon removal fluxes from BECCS as estimated by the IAMs were folded into net emissions variables (Gidden et al., 2019), which were then used to determine atmospheric CO_2 trajectories (Meinshausen et al., 2020). Even in the few emission-driven CMIP6 scenarios (Keller et al., 2018a), negative emissions from BECCS were prescribed to ESMs rather than simulated as originating from an explicit land-use activity, leading to inconsistencies in how land-use changes, ecosystem carbon pools, and CDR-related carbon fluxes are represented.

In the run-up to the 7th phase of the Coupled Model Intercomparison Project (CMIP7; Dunne et al., 2025) several authors have argued for a stronger focus on emission-driven simulations (Jones et al., 2024; Meinshausen et al., 2024; Sanderson et al., 2024), and the CMIP7 ScenarioMIP protocol (Van Vuuren et al., 2026) adopts this priority, albeit no activity-driven representation of CDR is foreseen. The main advantage of emission-driven over concentration-driven multi-model ensembles is that the former can represent the full range of Earth system responses, including all feedbacks, to emissions and also to CDR. However, how the effects and feedbacks of CDR can be quantified from emission-driven ESM simulations remains unclear.

Here, we argue that in addition to emission-driven ESM simulations of mitigation scenarios, no-CDR baselines are required to *i)* determine carbon-cycle feedbacks and biogeophysical effects of CDR and thereby the efficiency of CDR in such simulations, and *ii)* to assess the consistency of various IAM assumptions with activity-driven modelling of CDR in ESMs. We discuss different choices and challenges for the creation of no-CDR baselines and their implications (Sect. 3), and we lay out a simulation framework to achieve the goals *i)* and *ii)* (Sect. 4). We use four main categories of CDR to exemplify our simulation framework: BECCS, A/R, ocean alkalinity enhancement (OAE), and direct air carbon capture and storage (DACCS), but the ideas and challenges discussed here also apply to other CDR options. We present an example for the application of our simulation framework using a 1.5°C-compliant overshoot scenario that includes activity-driven simulation of OAE (Sect. 5). We finally present our conclusions and make recommendations for improving the representation of CDR in the IAM-ESM modelling chain (Sect. 6). We begin with providing more background and motivation for our work together with the definition of terminology used for our simulation framework (Sect. 2).

2. Motivation and definitions

Our work focuses on the IAM – ESM modelling chain that has been established for the assessment of future scenarios in ScenarioMIP over the past decades (O'Neill et al., 2016; Taylor et al., 2012; Van Vuuren et al., 2026). We aim at assessing the efficiency of CDR together with carbon-cycle feedbacks and biogeophysical effects caused by the deployment of CDR in mitigation scenarios. Understanding the Earth system response to CDR is multifaceted, and we do not intend to propose a framework that is suited or preferable for all research questions. We acknowledge that stylized experiments with ESMs or with land and ocean offline models are important for understanding CDR independently of socio-economic constraints. We also focus solely on the feedbacks caused by CDR deployment, which is distinct from determining carbon-cycle feedbacks in response to rising atmospheric CO_2 and to climate change in ESMs (e.g., Arora et al., 2020a).

2.1. Net atmospheric removal and process carbon removal

Carbon cycle feedbacks in the Earth system exert a major control on atmospheric CO_2 concentrations. Of every tonne of CO_2 emitted, terrestrial and oceanic sinks currently take up more than 0.5 tonnes (Friedlingstein et al., 2025). ESMs project that these sinks will take up less carbon under declining CO_2 emissions (e.g., Liddicoat et al., 2021; Terhaar, 2024), and potentially can be turned into a source of carbon under net-zero or net-negative emissions (e.g., Keller et al., 2018b; Koven et al., 2022; MacDougall et al., 2020; Oschlies, 2009; Schwinger et al., 2022; Smith et al., 2025). Hence, due to the buffering nature of carbon cycle feedbacks, the net atmospheric reduction of CO_2 in CDR scenarios will always be less than the gross amount of CO_2 that has been removed.

CDR methods that involve land-use changes (e.g. A/R, BECCS), will additionally cause local and non-local biogeophysical effects and feedbacks, for example, through changes in surface albedo, surface roughness, and evapotranspiration. Thereby, CDR can change the surface energy balance and atmospheric circulation patterns (Boysen et al., 2014, 2020; De Hertog et al., 2023; King et al., 2024). Such effects might in turn indirectly modify the carbon removal efficiency of BECCS and A/R (e.g. increasing drought and fire risk might diminish the carbon removal achieved by A/R), and they are highly relevant for the assessment of the impacts of CDR.

Here, we refer to the net removal of CO_2 from the atmosphere by CDR, including all effects and feedbacks (carbon-cycle and biogeophysical), as the *Net Atmospheric Removal* (NAR). More specifically, we define the NAR as the difference in atmospheric CO_2 content (in Pg C) between an emission-driven ESM scenario simulation S and a corresponding no-CDR baseline B (see below for a more detailed discussion of no-CDR baselines)

$$\Delta C^{NAR}(t) = C^{B}_{atm}(t) - C^{S}_{atm}(t), \quad (1)$$

where C_{atm} is the total mass of atmospheric carbon. At time *t*, the NAR reflects the accumulated effect of CDR including all feedbacks on atmospheric CO_2 up to time *t*. The NAR depends on the strength of terrestrial and oceanic carbon-cycle feedbacks and thereby on the emission pathway, since the terrestrial and oceanic carbon fluxes will evolve differently under a high-emission compared to a strong mitigation scenario. The NAR will even evolve after a CDR intervention has been stopped until the CDR effect on the carbon cycle has diminished.

Although the NAR is an important metric indicating the overall success or failure of CDR, it is not an intrinsic property of a given CDR method. It is neither a suitable metric for carbon accounting: In the same way emissions are priced per tonne of CO_2 emitted (disregarding the effect of sinks on atmospheric CO_2), carbon removals need to be accounted for without the effect of carbon cycle feedbacks. We therefore define the *process carbon removal* (PCR) as the net amount of carbon removed by a CDR process (removals minus positive emissions related to the process) without taking carbon-cycle feedbacks into account. This net amount of carbon removed is the quantity that IAMs estimate in the first place. For methods with geological storage of CO_2 (e.g., DACCS and BECCS), the PCR might be relatively straightforward to estimate, since we only need to subtract positive emissions related to DACCS and BECCS from the amount of carbon in geological storage.

However, for methods that enhance the storage of carbon in natural reservoirs (e.g., A/R and OAE), we need additional model simulations that switch off the effect of carbon-cycle feedbacks on these natural reservoirs. In ESMs we can mimic such behavior and determine the PCR by prescribing atmospheric CO_2 concentrations (Boysen et al., 2014; Oschlies, 2009; Schwinger et al., 2024; Tyka, 2025). We will provide a more specific definition of the PCR in Section 4.

In contrast to the NAR, the PCR allows a comparison between CDR methods with and without geological storage, and it allows comparing removals estimated by IAMs and simulated by ESMs. We note that both the PCR and NAR include biogeophysical effects of CDR interventions on climate and carbon storage. While the NAR is a global metric by definition (defined through total atmospheric CO_2 content in Eq. 1), a spatially explicit attribution of the PCR to specific CDR interventions is possible (Sect. 4). Both metrics depend on the atmospheric CO_2 pathway. For the NAR this is obvious, because of the contributions of carbon-cycle feedbacks, but also the PCR may depend on the atmospheric CO_2 pathway (Jürchott et al., 2023; Schwinger et al., 2024; Sonntag et al., 2016) and vary spatially (He and Tyka, 2023; Zhou et al., 2025).

Table 1: Overview of key CDR diagnostics of the IAM-ESM framework presented here. More details can be found in Section 4.

Term	Symbol	Definition used in this study	Notes
Net Atmospheric Removal (NAR)	ΔC^{NAR}	Net reduction in atmospheric CO_2 attributable to CDR, including all carbon-cycle feedbacks and biogeophysical effects, diagnosed as the difference in atmospheric carbon content between a CDR scenario and the corresponding no-CDR baseline.	Not an intrinsic property of a CDR method. Distinct from “net removed” or “stored” as used in MRV contexts.
Process Carbon Removal (PCR)	ΔC^{PCR}	Amount of CO_2 removed by CDR when carbon-cycle feedbacks are suppressed, diagnosed by comparing a CDR simulation to a concentration-driven no-CDR baseline that shares the same atmospheric CO_2 pathway as the simulation with CDR (Sect. 4).	Conceptually identical to what IAMs report as captured CO_2 and to “net removed” or “stored” as used in MRV contexts.
Carbon-cycle CDR feedback contribution	ΔC^{cc}	Change in land and ocean carbon pools that arises because CDR alters atmospheric CO_2 and climate, obtained as the difference between NAR and PCR components for land and ocean (Sect. 4).	Quantifies by how much carbon-cycle feedbacks dampen the net atmospheric effect of the PCR.

Biogeophysical effects and feedbacks	ΔX^{bgp}	Response to physical changes caused by CDR (e.g. albedo, roughness, evapotranspiration, circulation) that modify surface climate and can in turn affect carbon fluxes. $\Delta X^{bgp}$is the difference in any direct or derived ESM output between the CDR scenario and a concentration-driven no-CDR baseline (Sect. 4)	Their net impact on atmospheric CO_2 is included in both, NAR and PCR. Possible to quantify their contributions, but this might be computationally expensive as discussed in Section 5.

2.2 Activity-driven CDR in ESMs

CDR, particularly A/R and BECCS, has been an important ingredient in deep mitigation scenarios created by IAMs. At the same time, the plausibility of the magnitude of CDR in many IAM scenarios has been contested (e.g., Gambhir et al., 2019; Hansson et al., 2021; Heck et al., 2018). Among other criticisms, it has been pointed out that IAMs might overestimate the achievable CO_2 removal by neglecting the influences of climate change on the efficiency and permanence of land-based CDR. For example, increasing drought and fire frequencies (Anderegg et al., 2022) could make afforested areas a less efficient carbon reservoir than assumed in IAMs (Windisch et al., 2025). The land-use changes related to an expansion of bioenergy could lead to losses of soil carbon which might not be represented to the full extent in IAMs. The possibility to investigate the interactions between land-use changes, climate changes and the efficiency of land-based and ocean-based CDR options is a strong motivation for simulating the activity that leads to the removal of CO_2 from the atmosphere interactively in ESMs, which we, following Sanderson et al., (2024), refer to as *activity-driven CDR.*

In the current state-of-the-art set-up of the IAM-ESM modelling chain (Fig. 1a), negative and positive emission fluxes for each CDR method are estimated by the IAM and prescribed to the ESM as a net emission flux (referred to as *prescribed CDR*). The upcoming ScenarioMIP for CMIP7 (Van Vuuren et al., 2026) will use this set-up. An exception has always been A/R, which is included in the land-use and land cover change patterns that are passed from IAM to ESM, such that the ESM simulates the carbon and climate outcomes of the land-use changes related to A/R interactively without using the respective emissions and removal from the IAMs.

Activity-driven CDR (Fig. 1b) rather simulates the activity in ESMs that eventually removes CO_2 from the atmosphere. In the following two sub-sections, we discuss some general principles for activity-driven simulation of BECCS and OAE in the IAM-ESM modelling chain. For DACCS, there is no activity that could be meaningfully simulated by an ESM, and for such CDR methods we continue to use the CO_2 removal fluxes calculated by the IAM as indicated in Fig. 1b. As mentioned above A/R has always been simulated in an activity-driven fashion, with an established data-flow between IAM and ESM, which we will not discuss further here. The characteristics of activity-driven CDR simulation for our example CDR portfolio consisting of DACCS, A/R, BECCS, and OAE are summarized in Table 1.

We note that an activity-driven representation of CDR can also be implemented in a concentration-driven ESM set-up. The options "activity-driven/prescribed CDR" and "emission/concentration-driven model set-up" are mutually independent. In a concentration-driven ESM simulation, an activity-driven CDR implementation would not alter the atmospheric CO_2 concentration, but climate change would still affect the activity-driven CDR and carbon fluxes can be diagnosed. In fact, as discussed above, the simulation of A/R in concentration-driven CMIP5 and CMIP6 simulations has always been of this type. However, to take full advantage of an activity-driven CDR implementation, it is desirable to run the ESM in emission-driven mode, and we will assume this combination here.

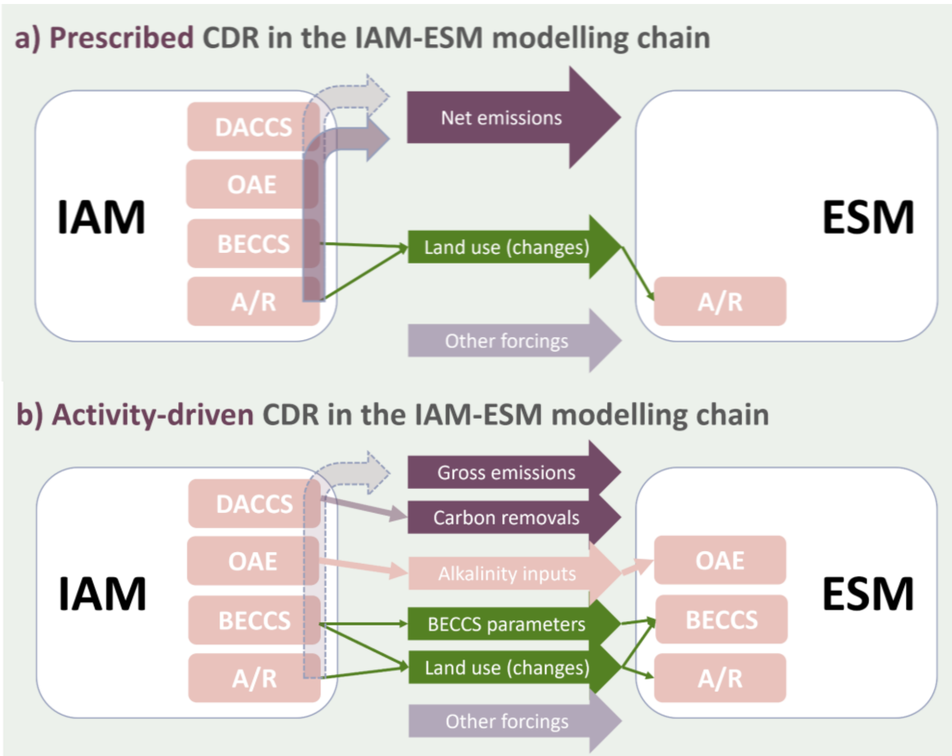

Figure 1: Schematic of (a) prescribed and (b) activity-driven CDR in the IAM-ESM modelling chain. Panel a depicts the current state-of-the-art, which has been used for CMIP5 and 6, and is planned for CMIP7. Panel (b) depicts activity-driven CDR as discussed in this paper.

2.2.1. Activity-driven BECCS

Bioenergy can be produced from different sources of biomass, from purpose-grown bioenergy crops and forest plantations, or from forestry residues among others. The details of how activity-driven simulation of BECCS can be implemented in ESMs will to some extent depend on this source. Here we focus on BECCS from purpose-grown energy crops, but we foresee that ESMs will diversify the flavours of BECCS that they are able to simulate in an activity-driven fashion.

Activity-driven BECCS from purpose-grown bioenergy crops is simulated by using the land-use pattern of bioenergy crops from the IAMs while simulating the crop yields endogenously within the ESMs. Typically (e.g., in ScenarioMIP), the land-use and land-cover change patterns are passed from IAM to ESM using the Land-Use Harmonization data set (LUH; Hurtt et al., 2020), which contains spatially explicit information on bioenergy crops. Given that all land-use and land-cover change patterns are input to the ESMs, this implicitly involves direct and also indirect land-use change from bioenergy that may lead to land-conversion in other parts of the world. Under insufficient land regulatory policies such land-use change can involve substantial emissions from clearing forests and other natural vegetation (Merfort et al. 2023). While bioenergy production typically expands strongly in deep mitigation scenarios, only a part of this bioenergy production is combined with CCS with the capture rate depending on the specific BECCS technology assumed (Bauer et al., 2020a). Furthermore, not all the captured CO_2 is stored geologically, as it can also be further used to, e.g., produce carbonaceous fuels (Carbon Capture and Utilization, CCU). Thus, only a part of the carbon embodied in the biomass is permanently injected into geological storage sites and that fraction may differ strongly between scenarios. For activity-driven implementation of BECCS in ESM this global-mean scenario- and time-dependent fraction is a key input that must be handed over from IAM to ESM.

However, biomass is a tradable good in IAMs (and in the real world), which makes it difficult to spatially attribute bioenergy crop production for use with CCS and for other uses. Some spatial information may be derived from the management information that is provided with the LUH-data. For example, the area attributable to BECCS can be constrained, if the IAM assumes that exclusively second-generation biofuel crops are combined with CCS. The fundamental problem that still only a fraction of these crops are used in combination with CCS remains. Therefore, in order to relate land-use patterns to BECCS we need to apply some heuristics. Here, we propose to assume that the amount of carbon stored geologically per unit of biomass harvested is homogeneous over the globe for all bioenergy crops (or a subset of bioenergy crops, e.g., second generation bioenergy crops). Hence, inputs provided by the IAM for activity simulation of BECCS are the land-use patterns for bioenergy crops and the global average amount of CO_2 that is stored geologically per unit of biomass harvested (given in $kgCO_2/tDM$, tDM=tonn of dry matter biomass). This storage ratio thus considers all the carbon flows from biomass harvest to geological storage, varies over time, and depends on the scenario assumptions. Emissions related to land-conversion are simulated by ESMs endogenously, but other gross positive emissions related to the production and processing of the biomass need to be provided by the IAM as a separate output, since these are not simulated by ESMs and need to be included in the emission forcing.

2.2.2 Activity-driven OAE

Activity-driven OAE is simulated through the addition of an alkaline agent to the surface ocean that alters the surface ocean chemistry and increases the carbon flux. Current implementations of OAE in IAMs (Kowalczyk et al. 2024; Strefler et al. 2025) assume the technique of *ocean liming*, i.e., the calcination of limestone to $Ca(OH)_2$ and subsequent distribution to the ocean using ships. Other proposed materials and techniques for OAE exist (see Renforth and Henderson 2017 for a review). To simulate activity-driven OAE, ESMs require a spatially explicit flux of alkalinity, which makes it necessary to spatially disaggregate the IAM-estimated production of alkaline materials. In general, this may require further assumptions on the deployment regions related to legal and governance issues. For example, materials can be distributed in the exclusive economic zones (EEZs) of the regions where they are produced, which is the approach taken for the OAE deployment examined in Section 5. Spatial disaggregation could also be further refined based on ecological thresholds in an iterative procedure between IAM scenario creation and activity-driven simulation of OAE in ESMs. If the material used for alkalinity addition also contains micro- and macro-nutrients or contaminants, these should also be provided by the IAM. For example, olivine contains silicates and iron, which have significant effects on ecosystems and carbon uptake upon addition to the surface ocean (Hauck et al., 2016). Finally, the gross positive CO_2 emissions related to the extraction, processing, and distribution of alkaline material, need to be provided by the IAM in order to include them in the emission forcing of the ESM.

Table 2: Summary of activity-driven CDR implementation in ESM

	ESM implementation	Data from IAM
DACCS	no activity-driven implementation, use net removal fluxes from IAM	n/a
A/R	Land use evolves according to IAM, removal is realized through changes in vegetation and soil carbon. A/R has been simulated in an activity-driven way in ESMs since CMIP5	Spatially explicit land use. Wood harvest and/or other management practices
BECCS	Land use evolves according to IAM, a fraction of harvested biomass is put into a CCS pool	Spatially explicit land use for bioenergy crops; global average amount of CO_2 stored geologically per unit of biomass harvested; other emissions related to biomass production
OAE	Flux of alkalinity applied to the surface ocean	Spatially explicit flux of total alkalinity at ocean surface; fluxes of nutrients or contaminants if applicable for the OAE technique; positive emissions from extraction, processing and distribution

2.3 no-CDR baseline

To assess the net effect of CDR on atmospheric CO_2 (NAR, Eq. 1), two emission-driven ESM simulations are needed, one that includes CDR and a *no-CDR baseline* where no CDR is deployed. The no-CDR baseline will lead to higher CO_2 concentrations and stronger climate warming, i.e., a climate target that is met in a given scenario will likely be missed in the corresponding no-CDR baseline. Otherwise (except for the omission of CDR), the no-CDR baseline is as similar as possible to the scenario simulation, i.e. emission reductions are pursued at the same level of ambition.

However, “switching off” CDR for the no-CDR baseline is not a well-defined operation, particularly if we move away from stylized simulations. In stylized ESM experiments it is, for example, possible to afforest huge land areas (De Hertog et al., 2023; Swann et al., 2012) without considering the socio-economic implications. The corresponding no-CDR baseline simulation would just omit this A/R. In contrast, in scenarios created by IAMs, the deployment of CDR is embedded in a consistent description of socio-economic and technological development, and A/R will compete with food and bioenergy production among other land uses. Even in the seemingly simple case of DACCS, a large-scale deployment of this energy-intensive CDR technology will have consequences for the energy sector (stronger competition), and through increased energy demand indirectly influence land-use demand for bioenergy. The same is true for OAE, which would require the energy-intensive production and distribution of large amounts of alkaline materials. Hence, while DACCS or activity-driven OAE can readily be 'switched off' in an ESM scenario simulation (by omitting the DACCS-related CO_2 removal and by not applying alkaline materials to the ocean), a consistent description of a world, in which DACCS or OAE had never been deployed, would look different. We will therefore discuss the creation of no-CDR baselines in more detail in the following section.

3. Ex-post and counterfactual no-CDR baselines

For the definition of the NAR (Eq. 1), we have introduced a no-CDR baseline, a simulation without CDR, consequently higher net CO_2 emissions, and more climate warming. Here, we introduce two different concepts for creating such baselines. First, to create the no-CDR baseline by ex-post adjustments of a given IAM scenario. With this option, CDR is, figuratively speaking, surgically removed from an existing IAM scenario (Sec. 3.1). Second, to create a new counterfactual IAM scenario without CDR, i.e. by inventing an alternative world without CDR ever being implemented (Sec. 3.2). From a technical point of view, the difference is that for the ex-post adjustments, we do not run the IAM again (we modify an existing IAM scenario), while for the counterfactual IAM scenario, we create a new scenario using the IAM. Here, we will discuss the counterfactual IAM scenario only briefly and qualitatively. The creation of such no-CDR baselines and comparison to the ex-post approach will be subject to future work.

The two options are complementary and methodologically very different, they offer different insights, and they have their specific limitations. For instance, A/R simulations may be used to ask the following question: "*What are the regional biogeophysical effects of A/R in a given scenario?*" To answer this question, we need to compare a scenario simulation including A/R to a simulation where the A/R pattern in the same location is not present. We might achieve this by ex-post adjustments to the IAM scenario, i.e. by "freezing" (see below for a more comprehensive definition) the land use in all grid cells that were planned for A/R. By doing so, we will, however, end up with a socio-economically inconsistent land-use pattern in the ex-post adjusted no-CDR baseline. If, for example, A/R happens on agricultural land in the original scenario, this area would just remain cropland in our ex-post adjusted scenario, and we would end up with more cropland than needed to secure food production. What is more, expansion of bioenergy and A/R can entail indirect, spatially remote land use changes (Merfort et al., 2023), and these indirectly mediated land use transitions cannot be frozen by the ex-post approach.

Alternatively, we could more generally ask "*How would two worlds differ when one uses A/R as a climate mitigation option and the other does not"?* This question could be answered with a counterfactual IAM no-CDR baseline. If we simulate such a no-CDR baseline with ESMs, we can analyze global scale carbon-cycle and biogeophysical feedbacks that are additionally informed by the socioeconomic feedback of not pursuing CDR (e.g. land not used for BECCS would be dedicated to other activities). Because the two land-use and land-cover change histories will be very different, such a counterfactual IAM no-CDR baseline is, however, not suited to determine localized effects and feedbacks of CDR.

3.1 Ex-post adjustments

3.1.1 DACCS and OAE

DACCS can be deactivated by omitting the prescribed net negative emission flux, while activity-driven OAE can be deactivated by omitting the fluxes of alkaline material to the ocean surface (Table 3). The IAM-estimated positive greenhouse gas emissions related to DACCS and to the extraction, processing, and distribution of materials for OAE, are also omitted in the no-CDR baseline.

In the original IAM scenario there might be indirect land-use changes caused by the energy-intensive DACCS and OAE technologies, because they alter the demand for carbon neutral energy from biomass. For OAE there is also the need for expansion of mining operations. However, we have no means of estimating and adjusting for these indirect land use changes ex-post. Therefore, we neglect such effects and propose to leave land-use patterns unchanged for the ex-post adjustments related to DACCS and OAE.

3.1.2 A/R

For A/R, the CO_2 uptake happens because of the conversion of non-forested land into forest, and subsequent expansion of vegetation and soil carbon pools. The biogeophysical and biogeochemical (carbon-cycle) effects and feedbacks of land cover changes in ESMs have been well studied, although the uncertainties remain large (e.g., Amali et al., 2025; Boysen et al., 2014, 2020; Brovkin et al., 2013; De Hertog et al., 2023; De Noblet-Ducoudré et al., 2012; Lawrence et al., 2016; Loughran et al., 2023; Moustakis et al., 2024). Many of these studies use a simulation where the land cover is "frozen" (i.e. it does not change over time) as a baseline, or they exchange the land-use patterns of a high A/R scenario with a less ambitious scenario.

Here, we are interested in isolating the effect of A/R in a given scenario, and we propose to use a more fine-grained "freezing"-approach for our ex-post no-CDR baseline. Two consecutive land-use states are connected through land-use transitions that specify the rates of conversion from one land-use type to another in each grid cell. Freezing a specific land-use state can be achieved by setting all corresponding transitions to zero. For the case of A/R, where we are interested in eliminating forest expansion (but not deforestation), we can also disable transitions to forest only, as illustrated in Fig. 2. In this case, land use is kept fixed at the state prior to A/R in grid-cells where forest area expands. All other land-use transitions including deforestation or conversion of primary forests to secondary (managed) forest are still allowed, such that our estimate of the CDR signal will not be biased by (artificially) avoided deforestation. As a complicating factor, there is the possibility that forest area may shrink towards the end of a scenario, for example, if afforested areas are not sufficiently protected by suitable policies (Merfort et al., 2023). To keep the land-use trajectory as close as possible to the original scenario for such cases, we propose to apply the deforestation land-use transitions proportionally to the land-use types that have remained fixed (i.e. that have replaced A/R), as illustrated in Fig 2. Whether or not this is necessary, depends on the scenario, and this step can be omitted if forest areas do not decrease significantly after A/R.

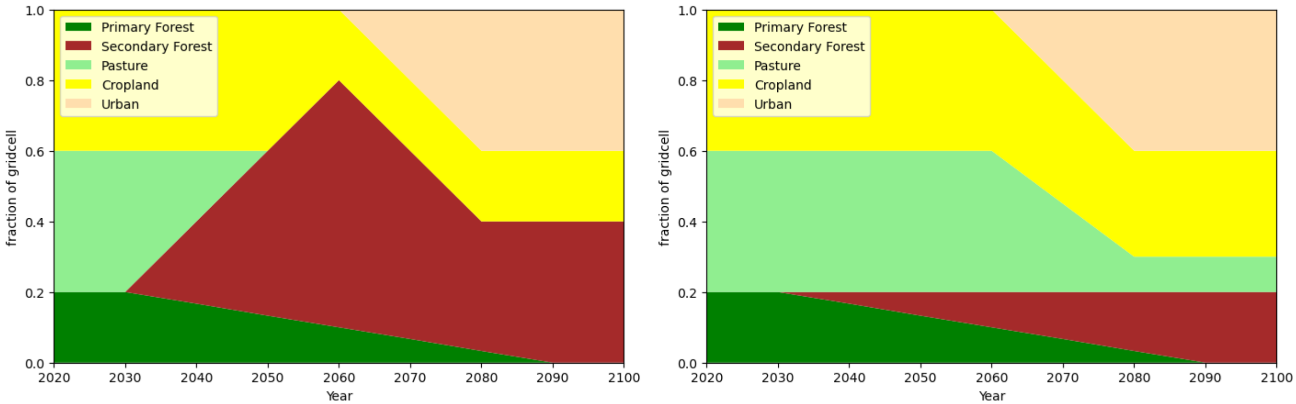

Figure 2: Schematic of a grid-cell undergoing A/R (left) and the proposed strategy for ex-post adjustments (right), where land-use transitions for A/R are "frozen". In this example forest area is reduced towards the end of the original A/R scenario, which is reflected by transitions of the "frozen" land use towards the land use that replaces the forest in the original scenario.

In the land-use forcing data for CMIP6 (LUH2; Hurtt et al., 2020) the "freezing"-approach implies that pre-CDR land cover fractions are maintained at grid-cells affected by A/R by removing the corresponding transitions to forest in transition files. Additionally, gross land-use transitions (i.e. sub-grid scale back- and forth-transitions between the same land-use/cover types) that exceed net changes should ideally be preserved (in ESMs that can handle such cases) to maintain realistic land-use dynamics. Indirect land use changes, i.e. transitions that are indirectly linked to A/R (e.g., expansion of agricultural area elsewhere) cannot be adjusted by ex-post "freezing" and must be neglected. Total *wood harvest* should be scaled down (in ESMs that handle this process) to preserve the per-hectare harvest intensity (carbon removed per area) of the original scenario in the no-CDR baseline, although it will depend on the ESM implementation of wood harvest if this can be achieved.

A/R can also happen unintentionally on abandoned land, for example in scenarios that assume a population peak and a decline towards the end of the century. These cases would not represent policy-driven A/R, and such unintentional regrowth should ideally not be conflated with policy-driven A/R by "freezing" the corresponding transitions in our no-CDR baseline. However, the LUH data for CMIP6 and CMIP7 does not offer a way to distinguish between the two cases. Since it seems reasonable to assume, as a first order approximation, that in scenarios with strong land-based mitigation, unintentional regrowth will contribute only little to total CDR, we will not distinguish between unintentional and policy-driven A/R. By doing so, we will overestimate the carbon removals achieved by policy-driven A/R, while the degree of overestimation will depend on the scenario (i.e., the amount of passive regrowth). As a side note, we mention that current reporting practices and recent assessments (e.g. Smith et al. 2024), do not make a distinction between passive regrowth and policy-driven A/R either.

3.1.3 BECCS

For BECCS, it is easy to “switch off” the CCS part of the technology and release the (otherwise stored) carbon back to the atmosphere. Additionally, the no-CDR baseline would ideally also eliminate the effects of the land conversion needed to provide the area for biomass production. However, compared to A/R, treating the land-use transitions for BECCS is much more difficult. Biomass is a tradable good, but IAMs in general do not trace back where the biomass that is used in combination with CCS was grown. Therefore, in current scenario frameworks, IAMs do not provide a spatially explicit land-use pattern for BECCS, only for bioenergy crops. For implementation of activity-driven BECCS, we have therefore proposed (Sect. 2.2) to use the global average amount of CO_2 stored geologically per unit of biomass harvested, which may vary over time. Using this information, we can attribute a fraction A of land used for bioenergy-crops (or a subset of bioenergy crop-types) to BECCS

$$A_{BECCS}(t) = A_{BE}(t)\, f_{BECCS}(t), \qquad (2)$$

where $f_{BECCS}(t)$ is the global average fraction of bioenergy crop yield used in combination with CCS. Changes in the land area used for BECCS can then be calculated as

$$\frac{d\,A_{BECCS}(t)}{dt} = A_{BE}(t)\,\frac{d\,f_{BECCS}(t)}{dt} + \frac{dA_{BE}(t)}{dt}\, f_{BECCS}(t) \qquad (3)$$

The first term on the right-hand side of Eq. 3 does not entail any land-use transition, since only f_{BECCS} changes. Therefore, the change in land area that entails land use transitions and can be attributed to BECCS is given by

$$\frac{d\,A_{BECSS,LUC}(t)}{dt} = \frac{dA_{BE}(t)}{dt} f_{BECCS}\,(t). \qquad (4)$$

Freezing the land-use transitions related to BECCS for the no-CDR baseline means to remove the part of the land use change that is attributable to BECCS from the total land use change related to bioenergy crops:

$$\frac{dA_{BE,frozen}(t)}{dt} = \frac{dA_{BE}(t)}{dt} - \frac{dA_{BECCS,LUC}\,(t)}{dt} = (1 - f_{BECCS}(t))\,\frac{dA_{BE}(t)}{dt} \qquad (5)$$

These considerations demonstrate that attributing land-use changes to BECCS is difficult in the current IAM-ESM modelling chain, because spatially explicit information on BECCS is missing. The use of Eq. 5 attributes BECCS-induced land-use changes proportionally and homogeneously to all bioenergy related land-use transitions and may thereby introduce regional biases in the estimated PCR of BECCS. Depending on the scenario, bioenergy expansion might happen on non-forested areas only, avoiding deforestation. In such cases, land-use change related carbon emissions will be small, and it might be justified to keep the land-use of the original scenario for the ex-post adjusted no-CDR baseline. However, in scenarios, where forests are not sufficiently protected, a significant replacement of forest by bioenergy crops might happen (Merfort et al., 2023). In such a case, the no-CDR baseline should freeze the BECCS-related land-use transitions according to Eq. 5.

3.1.4 Other considerations

For models with *dynamic vegetation* (dynamic biogeography), where the spatial distribution of natural vegetation evolves in response to environmental changes, we note that this feature can remain switched on in all simulations. By doing so, the feedback of CDR on the evolution of natural vegetation (e.g. on the poleward movement of the tree-line in high latitudes) is included in our estimate of NAR (consistent with the definition given above; NAR includes *all* feedbacks). In order to isolate signals from the CDR processes only (the PCR, excluding carbon cycle feedbacks), the amount of natural vegetated surface (that is not affected by A/R) must be kept the same for both the CDR scenario and the no-CDR baseline. In our simulation framework, this is achieved by running an additional concentration-driven no-CDR baseline (Boysen et al. 2014; see Sect. 4 for details), which has the same CO_2 concentration and climate as the scenario simulation and thus the same biogeography.

Table 3: Options to "switch off" CDR deployment by ex-post adjustments to IAM-created deep mitigation scenarios with CDR.

CDR	Ex-post "switch-off" option	Implications
DACCS	Assume no CO_2 is stored, negative emission flux provided by IAM is not applied in ESM; omit any greenhouse gas emissions related to DACCS (if any).	Energy system repercussions from an overall lower energy demand from disabling DACCS are not reflected. Particularly, changes in land-use dynamics due to a reduced bioenergy demand are not considered. Less competition for scarce CCS capacities is not reflected.
OAE	Alkaline material flux provided by IAM is not distributed to the ocean in ESM; omit process greenhouse gas emissions from the production and distribution of alkaline materials.	Energy system repercussions from an overall lower energy demand from disabling OAE are not reflected. Particularly, changes in land-use dynamics due to a reduced bioenergy demand and less mining operations are not considered. Less competition for scarce CCS capacities is not reflected.
BECCS	i) Assume that captured CO_2 is released back to atmosphere.	Land-use changes related to BECCS is ignored. Justifiable if bioenergy expansion happens on non-forested land

	ii) "Freeze" land-use transitions for BECCS as detailed in Eq. 2-5 and release captured CO_2 back to atmosphere.	Difficult to discriminate between bioenergy crops grown for BECCS and other bioenergy uses (e.g. biofuels). Indirect land-use change persists.
A/R	"Freeze" land-use transition to forested land.	Indirect land-use change persists. In scenarios with peak-and-decline forest area, treat frozen land use as described in Sect. 3.2.2. No distinction between passive regrowth and policy-driven A/R.

3.2 Counterfactual no-CDR baseline

Instead of applying ex-post adjustments to a given scenario, it is also possible to perform a second IAM simulation to create a *counterfactual* no-CDR baseline. Since our goal is to determine carbon-cycle and biogeophysical feedbacks, this counterfactual IAM-created no-CDR baseline needs to reflect a world where only emission reductions are pursued (at the same level of ambition as in the original scenario) but no CDR. This comes at the cost of higher net carbon emissions and higher temperatures.

This perspective on a no-CDR baseline has rarely been taken in the scenario literature so far, where the majority of CDR-related IAM studies is investigating the role of CDR in achieving a *given* climate target (e.g., Riahi et al., 2021; Strefler et al., 2021, 2025). In such studies, IAMs simulate scenarios that meet a given climate target (e.g., in terms of temperature or cumulative carbon emissions) with and without certain CDR methods. This design is targeted at investigating the socio-economic advantages or disadvantages in achieving the same climate target with or without CDR (or a certain CDR method), which implies that the net accumulated carbon emissions and resulting climate change remain very similar. In contrast, we are interested in the case where the omission of CDR as a mitigation option results in higher net carbon emissions and in a different climate.

For completeness, we provide a general recipe to construct such a counterfactual no-CDR baseline. We will, however, not provide a more detailed comparison of an ex-post and a counterfactual IAM scenario, since this is beyond the scope of the current paper. A counterfactual IAM no-CDR baseline can be created as follows: *(i)* Derive the amount of cumulative net CO_2 removals (net = gross removals minus positive emissions associated with a CDR method) over the whole simulation period in the IAM scenario. For example, the process emissions from OAE limestone calcination need to be removed from the CO_2 sequestration by the ocean; *(ii)* All other assumptions in the no-CDR baseline exactly resemble those in the CDR scenario except that the carbon budget is increased by the amount of cumulative net CDR derived in *(i)* and all CDR options are disabled. For example, if the original scenario had a carbon budget of 500 Gt CO_2 until the end of the century and 300 Gt CO_2 net removals, the "no-CDR" baseline would be a scenario with an 800 Gt CO_2 carbon budget until 2100, but with all CDR options disabled. This approach would avoid some of the problems with the ex-post adjustments discussed above, most importantly the problem of adjusting the land-use transitions for BECCS, but also indirect land-use changes related to other CDR methods. However, land use-patterns and the energy-system would be completely different between the scenario and the corresponding counterfactual no-CDR baseline. Regional biogeophysical effects could therefore not be assessed using this approach. Generally, the two approaches for generating no-CDR baselines deliver very different but complementary information. While the ex-post adjustments are targeted towards attribution, the counterfactual is suited to evaluate the socio-economic system response to a no-CDR assumption.

It is important to precisely define what “disabling” a certain CDR technology means. For example, “disabling BECCS” only means that the use of biomass in combination with *carbon sequestration* (CCS) is disabled, while the biomass could still be converted to a secondary carrier (e.g. electricity or liquid fuels), and even the waste CO_2 could be captured in order to use it for the production of synthetic fuels, as long as the captured CO_2 is eventually released to the atmosphere. The same is true for DACCS, where the direct air *capture* part could still be allowed in a no-CDR baseline to produce synthetic fuels if this is economically viable in the IAM.

4. Estimating feedbacks of CDR deployment from ESM scenario simulations using no-CDR baselines

The Net Atmospheric Removal (NAR) can be determined according to Eq. 1 from two emission-driven ESM simulations that simulate the carbon stocks of the Earth system with the respective CDRs enabled and disabled as described above. Whether the no-CDR baseline is created through ex-post adjustments to the original IAM scenario or whether it is a counterfactual IAM scenario has no implications for the simulation framework presented here, although the outcome of an analysis might differ, particularly for regional feedbacks.

We denote the ESM simulation of the original IAM scenario with activity-driven representation of CDR simulation S (Table 4). The emission-driven simulation of the no-CDR baseline (abbreviated B) will have higher atmospheric CO_2 concentrations and temperatures compared to simulation S. A given temperature limit, for example, the Paris Agreement’s 1.5°C limit, that might be achieved in S, is missed in B. The difference in atmospheric carbon content between B and S is the Net Atmospheric Removal (NAR) of CO_2 due to the portfolio of CDR options deployed in S and is directly obtained from the two emission-driven simulations (Eq. 1). This definition includes all effects and feedbacks (carbon cycle and biogeophysical) caused by the CDR deployment. The NAR can be decomposed into contributions from air-sea fluxes, from air-land fluxes and from fluxes directly out of the atmosphere into geological storage (DACCS):

$$\Delta C^{NAR}(t) = \Delta C_L^{NAR}(t) + \Delta C_O^{NAR}(t) + \Delta C_{DACCS}(t) \tag{6}$$

$$\Delta C_L^{NAR}(t) = \int_{t_o}^{t} (F_L^S - F_L^B)\ dt \tag{7}$$

$$\Delta C_O^{NAR}(t) = \int_{t_o}^{t} (F_O^S - F_O^B)\ dt \tag{8}$$

where F_L and F_O are the simulated air-land and air-sea carbon fluxes, respectively. Note that, as defined here, all ΔC are positive for carbon removal, since in this case the carbon fluxes in simulation S are larger than in B due to the land- and ocean-based CDR.

To estimate the process removal (PCR), we need an additional concentration-driven *no-CDR baseline* (Boysen et al., 2014; Schwinger et al., 2024; Tyka, 2025), which allows carbon-cycle feedbacks to be isolated. This simulation is also excluding all CDR (as simulation B), but it prescribes the atmospheric CO_2 trajectory from the full CDR scenario S. We denote this simulation B_S with the subscript indicating the simulation from which the atmospheric concentrations are prescribed. Thus, this simulation has the same atmosphere-ocean and atmosphere-land CO_2 fluxes as simulation S but without the contributions resulting from BECCS, A/R, and OAE. We can then define the accumulated PCR as

$$\Delta C_L^{PCR} = \int_{t_o}^{t} (F_L^S - F_L^{BS})\, dt = \Delta C_L^{NAR} + \Delta C_L^{cc} \qquad (9)$$

$$\Delta C_O^{PCR} = \int_{t_o}^{t} (F_O^S - F_O^{BS})\, dt = \Delta C_O^{NAR} + \Delta C_O^{cc} \qquad (10)$$

where the accumulated carbon-cycle-CDR feedback contributions are defined as:

$$\Delta C_L^{cc} = \int_{t_o}^{t} (F_L^B - F_L^{BS})\, dt \qquad (11)$$

$$\Delta C_O^{cc} = \int_{t_o}^{t} (F_O^B - F_O^{BS})\, dt \qquad (12)$$

For DACCS the process removal rate is known a priori (the amount of CO_2 transferred into geological storage minus positive emissions related to the process) and we do not need to estimate it. The PCR as defined here includes the biogeophysical effects on the carbon stocks, since it is calculated as the difference between S (including biogeophysical effects) and B_S (not including them). In contrast, our estimates of the carbon cycle feedback contributions ΔC^{cc} do not include any biogeophysical effects of CDR, since they are derived from two no-CDR baselines. We note that the carbon stored geologically through BECCS is included in ΔC_L^{PCR}, since it was part of $F_L^S(t)$.

The biogeophysical effects that are caused by CDR deployment, for example changes in surface temperature and precipitation due to A/R, can also be determined by comparing simulation S and B_S. Both simulations share the same atmospheric CO_2 trajectory, but simulation B_S does not include the land-use changes related to A/R and BECCS. Hence, the biogeophysical effect of CDR deployment for any direct or derived ESM output *X* can be calculated as

$$\Delta X^{bgc} = X^S - X^{BS}. \qquad (13)$$

However, as discussed in Sec. 3, the nature of the no-CDR baseline (counterfactual or ex-post adjustments) is critical for biogeophysical effects, particularly on the regional to continental scale.

There exists a slightly different way of defining the PCR (and consequently the carbon-cycle-CDR feedbacks) by using a simulation S_B that prescribes the atmospheric CO_2 concentration of simulation B to the CDR scenario S. This is detailed in Appendix A, but the definition given in Eq. 9 - 12 is preferable, since it defines the PCR along the trajectory of atmospheric CO_2 of simulations S.

Table 4: Simulations and model configurations needed to determine Earth system and process removals by CDR

	S	**B**	**B_S**
Model configuration	emission-driven	emission-driven	concentration-driven, atmospheric CO_2 concentration taken from S
CDR	activity-driven, land-use changes and OAE deployment according to IAM scenario	no-CDR baselines (Sect. 2.3 and 3)	

5. Illustration of removal and feedbacks of an OAE deployment scenario

To illustrate the modelling approach described in the previous sections, we use ESM simulations of a deep-mitigation scenario created by the REMIND-MAgPIE model (Bauer et al., 2023). REMIND-MAgPIE has been recently expanded to include ocean liming (a flavour of OAE, see e.g. Renforth and Henderson, 2017) as a CDR method (Kowalczyk et al., 2024; Strefler et al., 2025). The scenario considered here (Merfort et al., 2025) reaches an end-of-the-century carbon budget of 500 Gt CO_2 (from 2020), corresponding to a global warming level of 1.5°C in 2100, after a considerable overshoot. The peak cumulative carbon budget from 2020 reaches slightly more than 1000 Gt CO_2 around 2060 and is subsequently strongly reduced by a massive upscaling of CDR (BECCS, A/R, DACCS, and OAE).

We use the Norwegian Earth System Model NorESM2-LM (Seland et al., 2020; Tjiputra et al., 2020) to simulate this scenario with activity-driven implementation of OAE. A time-dependent and spatially explicit data set of OAE deployment has been produced as part of the IAM scenario output, which is used to prescribe the alkalinity input into the ocean. It is assumed that OAE is deployed within the exclusive economic zones (EEZs, but excluding polar regions). We simulate the no-CDR baselines (B and B_S) by omitting the alkalinity input as well as the process emissions of limestone calcination, which are provided as a separate IAM output. The energy-related emissions from production (other than the calcination emissions) and distribution of lime are not explicitly accounted for in the no-CDR baselines. These emissions are accounted for in the simulation S as part of the net industry emissions, but they have not been provided as a separate gross emission output such that they could be removed in the baseline simulations. Yet, these emissions should be rather small, given that most of the OAE activities only occur at high carbon prices, where the largest part of the energy system is already decarbonized. Note that in this example “no-CDR” refers to OAE only. We do not simulate BECCS in an activity-driven fashion but prescribe the negative BECCS emission from the IAM. Thereby all calculations are done for the OAE deployment only. For each of the simulations (S, B, and B_S) we have run 3 ensemble members, branching off three ensemble members of the NorESM2-LM CMIP6 emission-driven historical simulation.

The atmospheric CO_2 concentration (Fig. 3a) in S is smaller than in B due to the much larger air-sea CO_2-flux in S compared to B caused by the deployment of OAE (Fig. 3b). The difference in atmospheric CO_2 content (in PgC) is the NAR shown in panel d of Fig. 3. The PCR can be determined according to Eq. 10 as the difference between the ocean fluxes in simulations S and B_S, and the carbon-cycle-CDR feedback fluxes according to equations 11 and 12 as the difference between B and B_S. The land CO_2-flux in B_S would be expected to be identical to S in our example since we did not switch off any land-based CDR. This is not exactly the case due to internal variability in our model (and in the climate system), which is why there are spurious positive accumulated feedback contributions as long as the deployment is relatively small up to approximately 2080. Also, for the same reason, we see spuriously negative accumulated PCR and NAR values during the earlier phase of deployment. This issue is further discussed in Sec. 5.1.

For our simulated OAE deployment of 4.93 Pmol alkalinity (accumulated over the years 2050-2100, corresponding to 182.5 Gt $Ca(OH)_2$) , the accumulated PCR of 28.2 PgC by 2100 is reduced by 7.9 PgC (28%) due to land and ocean carbon-cycle feedbacks resulting in a NAR of 20.3 PgC. This corresponds to a reduction in atmospheric CO_2 of 9.7 ppm in 2100 due to the deployment of OAE. In NorESM2-LM, ocean and the terrestrial biosphere contribute about equally to the carbon-cycle-CDR feedback-fluxes (4.8 PgC for ocean, 3.1 PgC for land). However, all quantities calculated here are model-dependent and we expect, based on previous carbon-cycle feedback assessments (Arora et al., 2020b) that the land feedback-flux in particular might vary greatly between models.

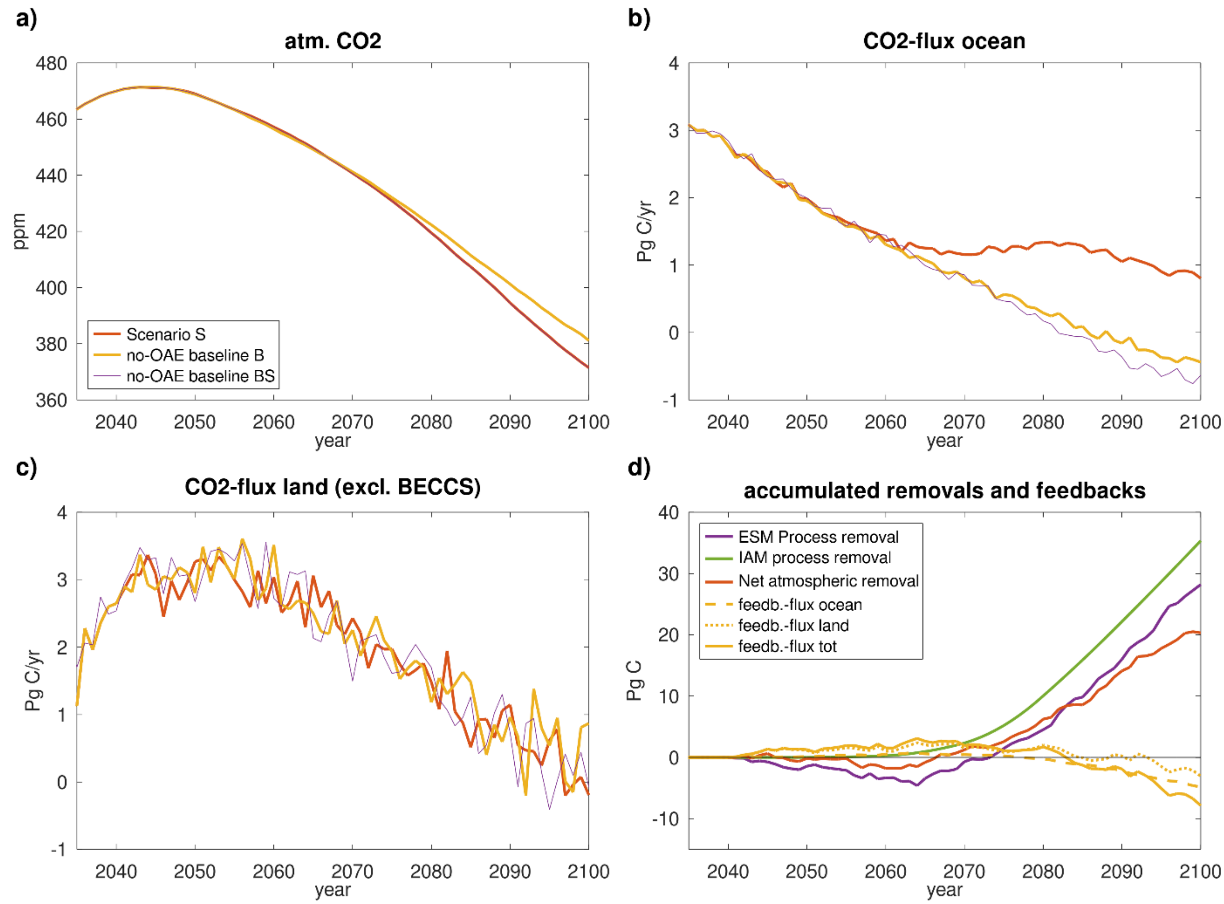

Figure 3: Estimating the net atmospheric and process carbon removals of OAE deployment in a deep mitigation scenario using the two no-CDR baselines B and B_S: Atmospheric CO_2 concentration (a), air-sea (b), and air-land (c) CO_2 fluxes in the emission-driven scenario S (red lines), the emission-driven no-CDR baseline B (yellow lines), and the concentration-driven no-CDR baseline B_S (atmospheric CO_2 concentrations from S prescribed, thin purple lines). The difference between the yellow and purple lines in panels b and c is used to derive the feedback contributions according to Eqs. 11 and 12, which is shown by the yellow lines in panel d. Panel d shows the accumulated net atmospheric and process carbon removals due to OAE as well as the accumulated feedback fluxes. The process carbon removal estimated by the IAM is also shown for comparison (line styles and colors as indicated in the legend in panel d).

An important aspect of simulating activity-driven CDR in ESMs is the possibility to compare the PCR simulated by the ESM with the PCR estimated by the IAM. REMIND-MAgPIE (and IAMs in general) have no ocean circulation model with carbonate chemistry to calculate the precise CO_2 drawdown per unit of alkalinity added. Instead, a constant efficiency of 0.57 mol CO_2 per mol alkalinity is assumed, whereas the efficiency of OAE is known to vary spatially (Zhou et al., 2025) and with the background scenario (Schwinger et al., 2024). Therefore, a comparison between the PCR assumed by the IAM with the PCR derived from the ESM with a full representation of all processes provides an important cross-check. In the case of our example scenario, the IAM accumulated PCR (green line in Fig. 3d) is larger by about 7.4 PgC (roughly 20%) in 2100 than the ESM PCR. Note that the IAM assumes instantaneous CO_2 sequestration upon addition of alkalinity, whereas in simulations with an ocean biogeochemistry model it takes up to 10-15 years until the full efficiency of an alkalinity addition has been reached (Zhou et al., 2025). Parts of the discrepancy between IAM and ESM will be caused by this simplification in the IAM, but our simulations provide no means of testing the exact amount of delayed OAE uptake in the ESM.

5.1. Internal variability

So far, we have ignored the problem of internal variability of the Earth system (e.g., Frölicher et al., 2016; Jain et al., 2023), which makes it practically difficult (or computationally expensive) to single out small signals from ESM simulations. The S-, B-, and B_S-simulations required to determine the NAR, the PCR, carbon-cycle-CDR feedbacks, and biogeophysical responses will not only be different in terms of their setup with respect to CDR and CO_2 coupling (summarized in Table 4), but will also quickly diverge from their common starting point with respect to modes of internal variability. CDR deployment in a scenario, even if it is at very small scales initially, acts as a perturbation relative to the no-CDR baselines. This has the same effect as a small perturbation of initial conditions, which is a technique utilized to create initial condition ensembles of ESM simulations. As shown in Fig. 4a, exemplified through the Niño-3.4 index, which indicates the phase of the El-Niño/Southern Oscillation (ENSO), the scenario simulation S and the no-CDR baseline B diverge immediately when the OAE deployment in S starts around the year 2040. After only a few years, the two simulations have reached a completely different state with respect to ENSO.

The different state with respect to modes of internal variability has implications for the CDR removals and feedback-fluxes calculated from these simulations according to Eq. 6 - 12 (Fig. 4b). Even the mean over the three ensemble members shows a variability that is comparable in magnitude with the global and annual mean signal over much of the scenario simulation. For the PCR in our example simulations, the noise level of natural variability remains significant (>0.25 Pg yr^{-1}) even for decadal averages (Fig. 4c, cyan vertical bars).

To avoid this problem, one could think of setting up the non-CDR baseline B_S as an offline simulation forced by the complete atmospheric state of S (instead of the atmospheric CO_2 concentration only). Thereby, $B_{S\text{-offline}}$ would be in the same state of internal variability as S, so the PCR could be determined cleanly from just one realization. However, our definition of the PCR intentionally includes biogeophysical effects (Eq. 9 and 10), and such effects would be suppressed by an offline simulation approach. This is most relevant for A/R, which changes surface temperature and humidity, as well as precipitation and circulation patterns, all of which might feed back on the PCR. Generally, for CDR methods that entail significant biogeophysical effects, the offline approach is not suitable, and the full assessment of the PCR requires a sufficiently large ensemble.

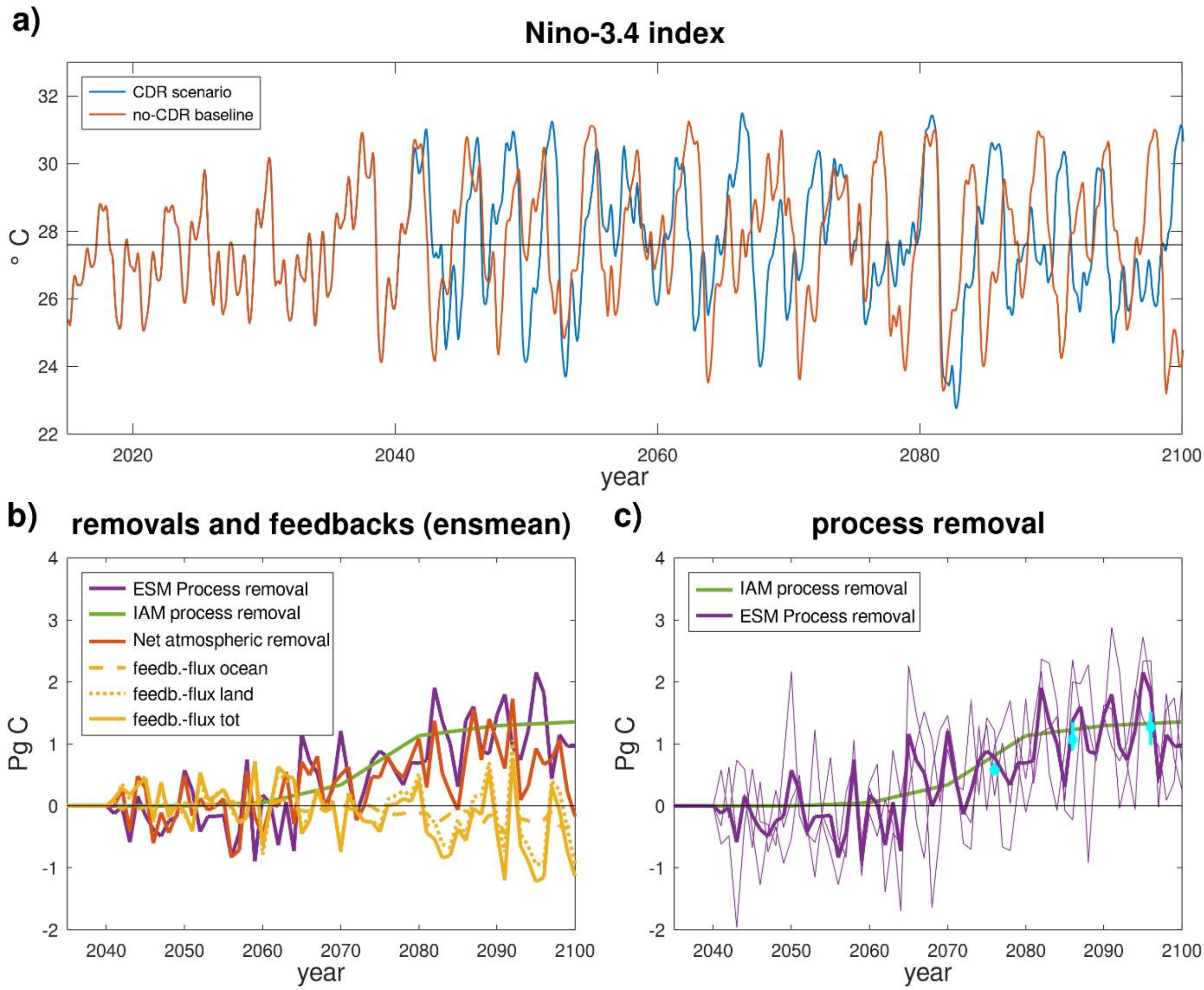

Figure 4: Niño-3.4 index for the scenario simulation S and the no-CDR baseline B (a), carbon removals and feedback fluxes (as indicated in the legend) calculated as the ensemble mean of three ensemble members of simulations S, B, and B_S (b), ensemble mean process removal (thick purple line) and individual ensemble members' process removal (thin purple lines) (c). The green lines in panels b and c show the process removal estimated by the IAM REMIND-MAgPIE for comparison. Cyan vertical bars in panel c indicate the range of the decadal mean PCR calculated from the three individual ensemble members.

6. Conclusions and recommendations

Activity-driven simulation of CDR in emission-driven ESMs allows to estimate the net atmospheric removal of CO_2 achieved by a portfolio of CDR methods (or a CDR method individually) in mitigation scenarios. This requires simulating a no-CDR baseline, a simulation where no CDR is deployed and net CO_2 emissions are higher by a corresponding amount. We have shown that the creation of such no-CDR baselines comes with challenges and trade-offs in the IAM-ESM modelling chain. For example, bioenergy crop cultivation typically expands strongly in deep-mitigation scenarios but only a fraction is coupled with CCS. Additionally, biomass is a tradable good and it is therefore difficult to attribute the carbon-cycle and biogeophysical effects of a given land conversion to BECCS on a local or regional level. More generally, we have pointed out that for CDR involving land-use transitions it is impossible to create a pair of simulations suitable to quantify regional carbon-cycle feedbacks and biogeophysical effects and maintain socio-economic consistency at the same time.

We have outlined two options for the creation of no-CDR baselines, to apply ex-post adjustments to a given IAM mitigation scenario, or to create a counterfactual scenario using the IAM. The two approaches are very different and deliver complementary information. The ex-post adjustments allow attributing effects of a specific CDR method down to a regional level at the cost of disregarding socio-economic consistency. In contrast, the counterfactual no-CDR baseline describes the system response to a no-CDR assumption in a socio-economic consistent way, but a regional attribution to specific CDR methods will not be possible. While approaches similar to the ex-post adjustments proposed here have been employed in previous studies, counterfactual no-CDR scenarios created by IAMs do not yet exist in the scenario literature to our knowledge. We believe it would be beneficial to compare the two approaches, and we recommend that IAM teams consider producing counterfactual no-CDR baselines for selected CDR scenarios in the future.

In order to compare the activity-driven removals simulated in ESMs with the removals estimated in IAMs, we additionally need simulations that exclude carbon-cycle-CDR feedbacks. We have discussed such concentration-driven no-CDR baseline simulations and presented an example where we compare the OAE process carbon removal estimated by an IAM with an activity-driven simulation of OAE in an ESM. We have shown that carbon-cycle-CDR feedbacks offset about 35% of the process removal by OAE in the scenario and ESM examined here. Both, carbon-cycle-CDR feedbacks and the simulated PCR are model- and scenario-dependent, and we therefore recommend applying our simulation protocol in future model intercomparison exercises that deal with activity-driven CDR, for example the next phase of CRDMIP in CMIP7 (Mengis et al. in prep.).

A fundamental problem for assessing the efficiency of CDR is the internal variability of the climate system. This is true for real-world monitoring, verification, and reporting, but also for purely model-based assessments as we have pointed out. Emission-driven simulations of CDR scenarios and no-CDR baselines do not only differ in their CDR deployment. We have shown that they diverge quickly with respect to modes of internal variability and behave like distinct ensemble members. Therefore, isolating the forced CDR-signal requires either large enough initial-condition ensembles, or averaging/accumulating the effect of CDR deployment over sufficiently long time periods. The PCR, specifically, could also be estimated through offline simulations employing the land or ocean component of an ESM, forced by the atmospheric state of the fully coupled scenario simulation. However, this is only viable if the biogeophysical effects of CDR are negligible, which will likely not be the case for methods with a large land-use footprint. We nevertheless recommend that ESM modelling groups develop and/or maintain the capability to force the land and ocean components of their ESM by the outputs of a fully coupled scenario simulation. More generally, our findings imply that emission-driven ESM simulations are not necessarily the best choice for all purposes. For example, concentration-prescribed land-atmosphere-only simulations might still be better suited to assess the local to regional scale biogeophysical effects of land conversions related to BECCS and A/R.

We have made recommendations for IAM outputs to be provided to ESMs for the activity-driven implementation of BECCS, A/R, and OAE (see Table 5 for a summary). In general, to facilitate activity-driven implementation of CDR in ESMs and for the no-CDR baselines, IAM scenario outputs should be made available at a sufficiently high level of disaggregation to allow for attributing emissions and removals to specific CDR options. In particular, the gross positive emissions estimated by the IAM for each CDR method should be made available explicitly, since these need to be included in the emission forcing of the ESMs and excluded in ex-post adjusted no-CDR baseline simulations. In general, providing detailed IAM output is beneficial as this might enable a stepwise implementation of activity-driven representation of CDR in ESMs. For example, an ESM might have an activity-driven implementation of BECCS but not of OAE. If gross positive and gross negative emissions are provided separately for BECCS and OAE, this ESM can then run with activity-driven BECCS but prescribed OAE. The same is true if a CDR method has different flavours. For example, IAM outputs for BECCS should be provided separately for BECCS sourced from energy crops, forest plantations, or residues. ESMs can then choose to implement a subset of those in an activity-driven fashion and use prescribed emissions otherwise.

In the current (CMIP6 and CMIP7) land use data, there is no spatially explicit information on BECCS, only on bioenergy crops in general, which might or might not be combined with CCS. This is a major problem for activity-driven simulation of BECCS, particularly for the attribution of land use change emissions simulated by ESMs to BECCS. We recommend that the IAM community works towards making available spatially explicit information on BECCS in the management files of future versions of the LUH data set. Likewise, LUH currently offers no way to distinguish passive forest regrowth from policy-driven A/R, which may lead to an overestimation of the effect of policy-driven A/R in our simulation framework. We therefore recommend extending future versions of the LUH management data by an indicator that allows flagging passive regrowth of forests.

For the upcoming CMIP7 ScenarioMIP (Van Vuuren et al., 2026) it has been decided to stick to prescribed simulation of CDR in ESMs. Hence, ESMs will use the negative net emissions estimated by IAMs and prescribe this emission flux in their emission-driven scenario simulations. As no-CDR baselines are not foreseen either, the assessment of CDR through ScenarioMIP ESM simulations will be limited. The next phase of the Carbon Dioxide Removal Model Intercomparison Project (CDRMIP; Mengis et al., in prep.) aims at contributing to closing this gap by proposing activity-driven simulations of deep-mitigation scenarios according to the simulation framework outlined in this work.

Table 5: Summary of IAM output data needed as input for activity-driven simulation of CDR in ESMs and the construction of no-CDR baselines.

	Data available in CMIP6 / CMIP7	**New data required for activity-driven representation of CDR in ESMs**
General (applies for all CDR methods)		• Separate data for gross removals and gross positive emissions related to each CDR method. Gross positive emissions need to be included in the emission forcing for the ESM in scenario simulation S, but need to be omitted for the no-CDR baselines B. Gross removals are needed to compare the PCR between IAM and ESM. • Separate data for all flavours of a specific CDR method considered in the IAM, e.g. BECCS sourced from bioenergy crops, forest plantations, or forestry residues. Enables stepwise implementation of activity-driven CDR in ESMs.
A/R	• spatially explicit land-cover change • forest management information (wood harvest)	• Spatially explicit information on policy-driven A/R versus passive regrowth added to a future version of LUH
BECCS	• spatially explicit distribution of 2nd generation bioenergy crops	• Either: global average BECCS ratio expressed as CO_2 stored per tonne of dry biomass harvested (kg CO_2/t(DM)) • or, preferably: spatially explicit fraction of bioenergy crops used in combination with BECCS, together with spatially explicit BECCS efficiency (kg CO_2 stored per tonne of dry biomass harvested) added to a future version of LUH
OAE		• Spatially explicit flux of alkalinity addition to the surface ocean, together with fluxes of micronutrients and contaminants if applicable

Appendix A: Alternative definition of the process removal

There exist two slightly different options for defining the PCR for land- and ocean-based CDR methods. In Sect. 4 we define the PCR along the trajectory of atmospheric CO_2 of the CDR scenario S (Eq. 9 and 10). We could also define $\widehat{PCR}$ along the CO_2 trajectory of the non-CDR state in simulation B. To do so, we use the scenario simulation S with all CDR active, but we prescribe the atmospheric CO_2 concentration of the no-CDR baseline B (Table A1). Using this simulation S_B we define $\widehat{PCR}$ as

$$\Delta C_L^{\widehat{PCR}} \coloneqq \int_{t_o}^{t} (F_L^{SB} - F_L^{B})\, dt \;=\; \Delta C_L^{NAR} + \Delta C_L^{\widehat{cc}} \qquad \text{(A1)}$$

$$\Delta C_O^{\widehat{PCR}} \coloneqq \int_{t_o}^{t} (F_O^{SB} - F_O^{B})\, dt \;=\Delta C_O^{NAR} + \Delta C_O^{\widehat{cc}} \qquad \text{(A2)}$$

This alternative definition can be understood as evaluating the PCR along a different background state of the climate-carbon system, i.e. for different atmospheric CO_2 pathways and climatic conditions. If the PCR was independent of the atmospheric background CO_2 concentration, both definitions would be equivalent. However, the efficiency of CDR can depend on the atmospheric background (e.g. CO_2 fertilization for A/R, chemical effects on OAE). As the simulated CDR in S will see the atmospheric CO_2 concentration of S and not B, we prefer the definition of PCR given in the main text.

Since the NAR is defined the same way for both options, we also get a slightly different interpretation of the of the carbon-cycle-CDR feedback contributions $\Delta C^{\widehat{cc}}$:

$$\Delta C_L^{\widehat{cc}} = \int_{t_o}^{t} (F_L^{SB} - F_L^{S})\; dt \qquad \text{(A3)}$$

$$\Delta C_O^{\widehat{cc}} = \int_{t_o}^{t} (F_O^{SB} - F_O^{S})\, dt \qquad \text{(A4)}$$

These contributions are now defined with active CDR, while the $\Delta C_{L/O}^{cc}$(Eq. 11 and 12) are defined for the non-CDR state. If all four simulations listed in Table A1 are performed, it would theoretically be possible to determine the changes in carbon-cycle feedbacks due to CDR deployment as

$$\Delta C^{\widehat{cc}} - \Delta C^{cc} \;=\; \int_{t_o}^{t} (F^{Sb} - F^{S}) - (F^{B} - F^{Bs})\, dt \qquad \text{(A5)}$$

However, as pointed out in Sect. 5.1, a large number of ensemble members will be required to isolate small signals from these simulations.

Table A1: Full suite of simulations and model configurations to determine Earth system and process removals by CDR. S denotes the scenario simulation with activated CDR, B denotes the no-CDR baseline. Subscripts S/B indicate that the simulation is *concentration driven* with the concentration taken from the simulation S/B. Simulations without subscripts are *emission-driven*.

	S	**S_B**	**B**	**B_S**
Model configuration	emission-driven	concentration-driven, atmospheric CO_2 concentration from **B**	emission-driven	concentration-driven, atmospheric CO_2 concentration from **S**
CDR	activity-driven, land-use changes and OAE deployment according to IAM scenario		no-CDR baselines (all CDR switched off)	

Code and data availability

The source code of NorESM2 is available at https://doi.org/10.5281/zenodo.3905091 (Seland et al., 2020b). The model data generated in this study are available through the Norwegian Research Data Archive/Bjerknes Climate Data Centre and can be accessed at https://doi.org/10.11582/2025.XXXXX (Schwinger and Bourgeois, 2026).

Author contributions

This study was conceptualized by all authors. JS wrote the manuscript with contributions from all co-authors. LM, NB, PS, MJG, and ET created and prepared the scenario input data for running NorESM2-LM. JS and TB carried out NorESM2-LM simulations and analysed the results. All authors reviewed and commented on early versions of the manuscript.

Competing interests

The contact author has declared that none of the authors has any competing interests.

Disclaimer

Views and opinions expressed in this text are those of the authors only and do not necessarily reflect those of the European Union or European Research Executive Agency. Neither the European Union nor the granting authority can be held responsible for them.

Acknowledgements

Supercomputing and storage resources for NorESM2-LM simulations were provided by UNINETT Sigma2 (projects nn10054k/ns10054k). MJG is also affiliated with Pacific Northwest National Laboratory, which did not provide specific support for this paper. The authors thank Irina Melnikowa and Ben Sanderson for their constructive reviews, which helped improving our paper.

Financial support

This work was funded by the European Union through the Horizon Europe Framework Programme, project RESCUE (grant no. 101056939) and OptimESM (grant no. 101081193). JS and HM were also supported by the Research Council of Norway through the project NorESM4CMIP7 (grant no. 352204). N.M. is funded under the Emmy Noether scheme by the German Research Foundation (DFG) in the project 'FOOTPRINTS - From carbOn remOval To achieving the PaRIs agreemeNt's goal: Temperature Stabilisation' (ME 5746/1-1).

Review statement

References

Amali, A. A., Schwingshackl, C., Ito, A., Barbu, A., Delire, C., Peano, D., Lawrence, D. M., Wårlind, D., Robertson, E., Davin, E. L., Shevliakova, E., Harman, I. N., Vuichard, N., Miller, P. A., Lawrence, P. J., Ziehn, T., Hajima, T., Brovkin, V., Zhang, Y., Arora, V. K., and Pongratz, J.: Biogeochemical versus biogeophysical temperature effects of historical land-use change in CMIP6, Earth Syst. Dynam., 16, 803–840, https://doi.org/10.5194/esd-16-803-2025, 2025.

Anderegg, W. R. L., Wu, C., Acil, N., Carvalhais, N., Pugh, T. A. M., Sadler, J. P., and Seidl, R.: A climate risk analysis of Earth's forests in the 21st century, Science, 377, 1099–1103, https://doi.org/10.1126/science.abp9723, 2022.

Arora, V. K., Katavouta, A., Williams, R. G., Jones, C. D., Brovkin, V., Friedlingstein, P., Schwinger, J., Bopp, L., Boucher, O., Cadule, P., Chamberlain, M. A., Christian, J. R., Delire, C., Fisher, R. A., Hajima, T., Ilyina, T., Joetzjer, E., Kawamiya, M., Koven, C. D., Krasting, J. P., Law, R. M., Lawrence, D. M., Lenton, A., Lindsay, K., Pongratz, J., Raddatz, T., Séférian, R., Tachiiri, K., Tjiputra, J. F., Wiltshire, A., Wu, T., and Ziehn, T.: Carbon–concentration and carbon–climate feedbacks in CMIP6 models and their comparison to CMIP5 models, Biogeosciences, 17, 4173–4222, https://doi.org/10.5194/bg-17-4173-2020, 2020a.

Arora, V. K., Katavouta, A., Williams, R. G., Jones, C. D., Brovkin, V., Friedlingstein, P., Schwinger, J., Bopp, L., Boucher, O., Cadule, P., Chamberlain, M. A., Christian, J. R., Delire, C., Fisher, R. A., Hajima, T., Ilyina, T., Joetzjer, E., Kawamiya, M., Koven, C. D., Krasting, J. P., Law, R. M., Lawrence, D. M., Lenton, A., Lindsay, K., Pongratz, J., Raddatz, T., Séférian, R., Tachiiri, K., Tjiputra, J. F., Wiltshire, A., Wu, T., and Ziehn, T.: Carbon–concentration and carbon–climate feedbacks in CMIP6 models and their comparison to CMIP5 models, Biogeosciences, 17, 4173–4222, https://doi.org/10.5194/bg-17-4173-2020, 2020b.

Bauer, N., Rose, S. K., Fujimori, S., Van Vuuren, D. P., Weyant, J., Wise, M., Cui, Y., Daioglou, V., Gidden, M. J., Kato, E., Kitous, A., Leblanc, F., Sands, R., Sano, F., Strefler, J., Tsutsui, J., Bibas, R., Fricko, O., Hasegawa, T., Klein, D., Kurosawa, A., Mima, S., and Muratori, M.: Global energy sector emission reductions and bioenergy use: overview of the bioenergy demand phase of the EMF-33 model comparison, Climatic Change, 163, 1553–1568, https://doi.org/10.1007/s10584-018-2226-y, 2020a.

Bauer, N., Bertram, C., Schultes, A., Klein, D., Luderer, G., Kriegler, E., Popp, A., and Edenhofer, O.: Quantification of an efficiency–sovereignty trade-off in climate policy, Nature, 588, 261–266, https://doi.org/10.1038/s41586-020-2982-5, 2020b.

Bauer, N., Keller, D. P., Garbe, J., Karstens, K., Piontek, F., Von Bloh, W., Thiery, W., Zeitz, M., Mengel, M., Strefler, J., Thonicke, K., and Winkelmann, R.: Exploring risks and benefits of overshooting a 1.5 °C carbon budget over space and time, Environ. Res. Lett., 18, 054015, https://doi.org/10.1088/1748-9326/accd83, 2023.

Bergero, C., Wise, M., Lamers, P., Wang, Y., and Weber, M.: Biochar as a carbon dioxide removal strategy in integrated long-run mitigation scenarios, Environ. Res. Lett., 19, 074076, https://doi.org/10.1088/1748-9326/ad52ab, 2024.

Boucher, O., Halloran, P. R., Burke, E. J., Doutriaux-Boucher, M., Jones, C. D., Lowe, J., Ringer, M. A., Robertson, E., and Wu, P.: Reversibility in an Earth System model in response to CO2 concentration changes, Environ. Res. Lett., 7, 024013, https://doi.org/10.1088/1748-9326/7/2/024013, 2012.

Boysen, L. R., Brovkin, V., Arora, V. K., Cadule, P., De Noblet-Ducoudré, N., Kato, E., Pongratz, J., and Gayler, V.: Global and regional effects of land-use change on climate in 21st century simulations with interactive carbon cycle, Earth Syst. Dynam., 5, 309–319, https://doi.org/10.5194/esd-5-309-2014, 2014.

Boysen, L. R., Brovkin, V., Pongratz, J., Lawrence, D. M., Lawrence, P., Vuichard, N., Peylin, P., Liddicoat, S., Hajima, T., Zhang, Y., Rocher, M., Delire, C., Séférian, R., Arora, V. K., Nieradzik, L., Anthoni, P., Thiery, W., Laguë, M. M., Lawrence, D., and Lo, M.-H.: Global climate response to idealized deforestation in CMIP6 models, Biogeosciences, 17, 5615–5638, https://doi.org/10.5194/bg-17-5615-2020, 2020.

Brovkin, V., Boysen, L., Arora, V. K., Boisier, J. P., Cadule, P., Chini, L., Claussen, M., Friedlingstein, P., Gayler, V., Van Den Hurk, B. J. J. M., Hurtt, G. C., Jones, C. D., Kato, E., De Noblet-Ducoudré, N., Pacifico, F., Pongratz, J., and Weiss, M.: Effect of Anthropogenic Land-Use and Land-Cover Changes on Climate and Land Carbon Storage in CMIP5 Projections for the Twenty-First Century, Journal of Climate, 26, 6859–6881, https://doi.org/10.1175/JCLI-D-12-00623.1, 2013.

Buck, H. J., Carton, W., Lund, J. F., and Markusson, N.: Why residual emissions matter right now, Nat. Clim. Chang., 13, 351–358, https://doi.org/10.1038/s41558-022-01592-2, 2023.

De Hertog, S. J., Havermann, F., Vanderkelen, I., Guo, S., Luo, F., Manola, I., Coumou, D., Davin, E. L., Duveiller, G., Lejeune, Q., Pongratz, J., Schleussner, C.-F., Seneviratne, S. I., and Thiery, W.: The biogeophysical effects of idealized land cover and land management changes in Earth system models, Earth Syst. Dynam., 14, 629–667, https://doi.org/10.5194/esd-14-629-2023, 2023.

De Noblet-Ducoudré, N., Boisier, J.-P., Pitman, A., Bonan, G. B., Brovkin, V., Cruz, F., Delire, C., Gayler, V., Van Den Hurk, B. J. J. M., Lawrence, P. J., Van Der Molen, M. K., Müller, C., Reick, C. H., Strengers, B. J., and Voldoire, A.:

Determining Robust Impacts of Land-Use-Induced Land Cover Changes on Surface Climate over North America and Eurasia: Results from the First Set of LUCID Experiments, J. Climate, 25, 3261–3281, https://doi.org/10.1175/JCLI-D-11-00338.1, 2012.

Dunne, J. P., Hewitt, H. T., Arblaster, J. M., Bonou, F., Boucher, O., Cavazos, T., Dingley, B., Durack, P. J., Hassler, B., Juckes, M., Miyakawa, T., Mizielinski, M., Naik, V., Nicholls, Z., O'Rourke, E., Pincus, R., Sanderson, B. M., Simpson, I. R., and Taylor, K. E.: An evolving Coupled Model Intercomparison Project phase 7 (CMIP7) and Fast Track in support of future climate assessment, Geosci. Model Dev., 18, 6671–6700, https://doi.org/10.5194/gmd-18-6671-2025, 2025.

Egerer, S., Falk, S., Mayer, D., Nützel, T., Obermeier, W. A., and Pongratz, J.: How to measure the efficiency of bioenergy crops compared to forestation, Biogeosciences, 21, 5005–5025, https://doi.org/10.5194/bg-21-5005-2024, 2024.

Eyring, V., Bony, S., Meehl, G. A., Senior, C. A., Stevens, B., Stouffer, R. J., and Taylor, K. E.: Overview of the Coupled Model Intercomparison Project Phase 6 (CMIP6) experimental design and organization, Geosci. Model Dev., 9, 1937–1958, https://doi.org/10.5194/gmd-9-1937-2016, 2016.

Friedlingstein, P., O'Sullivan, M., Jones, M. W., Andrew, R. M., Hauck, J., Landschützer, P., Le Quéré, C., Li, H., Luijkx, I. T., Olsen, A., Peters, G. P., Peters, W., Pongratz, J., Schwingshackl, C., Sitch, S., Canadell, J. G., Ciais, P., Jackson, R. B., Alin, S. R., Arneth, A., Arora, V., Bates, N. R., Becker, M., Bellouin, N., Berghoff, C. F., Bittig, H. C., Bopp, L., Cadule, P., Campbell, K., Chamberlain, M. A., Chandra, N., Chevallier, F., Chini, L. P., Colligan, T., Decayeux, J., Djeutchouang, L. M., Dou, X., Duran Rojas, C., Enyo, K., Evans, W., Fay, A. R., Feely, R. A., Ford, D. J., Foster, A., Gasser, T., Gehlen, M., Gkritzalis, T., Grassi, G., Gregor, L., Gruber, N., Gürses, Ö., Harris, I., Hefner, M., Heinke, J., Hurtt, G. C., Iida, Y., Ilyina, T., Jacobson, A. R., Jain, A. K., Jarníková, T., Jersild, A., Jiang, F., Jin, Z., Kato, E., Keeling, R. F., Klein Goldewijk, K., Knauer, J., Korsbakken, J. I., Lan, X., Lauvset, S. K., Lefèvre, N., Liu, Z., Liu, J., Ma, L., Maksyutov, S., Marland, G., Mayot, N., McGuire, P. C., Metzl, N., Monacci, N. M., Morgan, E. J., Nakaoka, S.-I., Neill, C., Niwa, Y., Nützel, T., Olivier, L., Ono, T., Palmer, P. I., Pierrot, D., Qin, Z., Resplandy, L., Roobaert, A., Rosan, T. M., Rödenbeck, C., Schwinger, J., Smallman, T. L., Smith, S. M., Sospedra-Alfonso, R., Steinhoff, T., et al.: Global Carbon Budget 2024, Earth Syst. Sci. Data, 17, 965–1039, https://doi.org/10.5194/essd-17-965-2025, 2025.

Frölicher, T. L., Rodgers, K. B., Stock, C. A., and Cheung, W. W. L.: Sources of uncertainties in 21st century projections of potential ocean ecosystem stressors, Global Biogeochemical Cycles, 30, 1224–1243, https://doi.org/10.1002/2015GB005338, 2016.

Fuhrman, J., Bergero, C., Weber, M., Monteith, S., Wang, F. M., Clarens, A. F., Doney, S. C., Shobe, W., and McJeon, H.: Diverse carbon dioxide removal approaches could reduce impacts on the energy–water–land system, Nat. Clim. Chang., 13, 341–350, https://doi.org/10.1038/s41558-023-01604-9, 2023.

Gambhir, A., Butnar, I., Li, P.-H., Smith, P., and Strachan, N.: A Review of Criticisms of Integrated Assessment Models and Proposed Approaches to Address These, through the Lens of BECCS, Energies, 12, 1747, https://doi.org/10.3390/en12091747, 2019.

Gidden, M. J., Riahi, K., Smith, S. J., Fujimori, S., Luderer, G., Kriegler, E., Van Vuuren, D. P., Van Den Berg, M., Feng, L., Klein, D., Calvin, K., Doelman, J. C., Frank, S., Fricko, O., Harmsen, M., Hasegawa, T., Havlik, P., Hilaire, J., Hoesly, R., Horing, J., Popp, A., Stehfest, E., and Takahashi, K.: Global emissions pathways under different socioeconomic scenarios for use in CMIP6: a dataset of harmonized emissions trajectories through the end of the century, Geosci. Model Dev., 12, 1443–1475, https://doi.org/10.5194/gmd-12-1443-2019, 2019.

Gidden, M. J., Brutschin, E., Ganti, G., Unlu, G., Zakeri, B., Fricko, O., Mitterrutzner, B., Lovat, F., and Riahi, K.: Fairness and feasibility in deep mitigation pathways with novel carbon dioxide removal considering institutional capacity to mitigate, Environ. Res. Lett., 18, 074006, https://doi.org/10.1088/1748-9326/acd8d5, 2023.

Hansson, A., Anshelm, J., Fridahl, M., and Haikola, S.: Boundary Work and Interpretations in the IPCC Review Process of the Role of Bioenergy With Carbon Capture and Storage (BECCS) in Limiting Global Warming to 1.5°C, Front. Clim., 3, 643224, https://doi.org/10.3389/fclim.2021.643224, 2021.

Hauck, J., Köhler, P., Wolf-Gladrow, D., and Völker, C.: Iron fertilisation and century-scale effects of open ocean dissolution of olivine in a simulated CO_2 removal experiment, Environ. Res. Lett., 11, 024007, https://doi.org/10.1088/1748-9326/11/2/024007, 2016.

He, J. and Tyka, M. D.: Limits and CO_2 equilibration of near-coast alkalinity enhancement, Biogeosciences, 20, 27–43, https://doi.org/10.5194/bg-20-27-2023, 2023.

Heck, V., Gerten, D., Lucht, W., and Popp, A.: Biomass-based negative emissions difficult to reconcile with planetary boundaries, Nature Clim Change, 8, 151–155, https://doi.org/10.1038/s41558-017-0064-y, 2018.

Hurtt, G. C., Chini, L., Sahajpal, R., Frolking, S., Bodirsky, B. L., Calvin, K., Doelman, J. C., Fisk, J., Fujimori, S., Klein Goldewijk, K., Hasegawa, T., Havlik, P., Heinimann, A., Humpenöder, F., Jungclaus, J., Kaplan, J. O., Kennedy, J., Krisztin, T., Lawrence, D., Lawrence, P., Ma, L., Mertz, O., Pongratz, J., Popp, A., Poulter, B., Riahi, K., Shevliakova, E., Stehfest, E., Thornton, P., Tubiello, F. N., Van Vuuren, D. P., and Zhang, X.: Harmonization of global land use change and management for the period 850–2100 (LUH2) for CMIP6, Geosci. Model Dev., 13, 5425–5464, https://doi.org/10.5194/gmd-13-5425-2020, 2020.

Jain, S., Scaife, A. A., Shepherd, T. G., Deser, C., Dunstone, N., Schmidt, G. A., Trenberth, K. E., and Turkington, T.: Importance of internal variability for climate model assessment, npj Clim Atmos Sci, 6, 68, https://doi.org/10.1038/s41612-023-00389-0, 2023.

Jones, C. G., Adloff, F., Booth, B. B. B., Cox, P. M., Eyring, V., Friedlingstein, P., Frieler, K., Hewitt, H. T., Jeffery, H. A., Joussaume, S., Koenigk, T., Lawrence, B. N., O'Rourke, E., Roberts, M. J., Sanderson, B. M., Séférian, R., Somot, S., Vidale, P. L., Van Vuuren, D., Acosta, M., Bentsen, M., Bernardello, R., Betts, R., Blockley, E., Boé, J., Bracegirdle, T., Braconnot, P., Brovkin, V., Buontempo, C., Doblas-Reyes, F., Donat, M., Epicoco, I., Falloon, P., Fiore, S., Frölicher, T., Fučkar, N. S., Gidden, M. J., Goessling, H. F., Graversen, R. G., Gualdi, S., Gutiérrez, J. M., Ilyina, T., Jacob, D., Jones, C. D., Juckes, M., Kendon, E., Kjellström, E., Knutti, R., Lowe, J., Mizielinski, M., Nassisi, P., Obersteiner, M., Regnier, P., Roehrig, R., Salas Y Mélia, D., Schleussner, C.-F., Schulz, M., Scoccimarro, E., Terray, L., Thiemann, H., Wood, R. A., Yang, S., and Zaehle, S.: Bringing it all together: science priorities for improved understanding of Earth system change and to support international climate policy, Earth Syst. Dynam., 15, 1319–1351, https://doi.org/10.5194/esd-15-1319-2024, 2024.

Jürchott, M., Oschlies, A., and Koeve, W.: Artificial Upwelling—A Refined Narrative, Geophysical Research Letters, 50, e2022GL101870, https://doi.org/10.1029/2022GL101870, 2023.

Keller, D. P., Feng, E. Y., and Oschlies, A.: Potential climate engineering effectiveness and side effects during a high carbon dioxide-emission scenario, Nat Commun, 5, 3304, https://doi.org/10.1038/ncomms4304, 2014.

Keller, D. P., Lenton, A., Scott, V., Vaughan, N. E., Bauer, N., Ji, D., Jones, C. D., Kravitz, B., Muri, H., and Zickfeld, K.: The Carbon Dioxide Removal Model Intercomparison Project (CDRMIP): rationale and experimental protocol for CMIP6, Geosci. Model Dev., 11, 1133–1160, https://doi.org/10.5194/gmd-11-1133-2018, 2018a.

Keller, D. P., Lenton, A., Littleton, E. W., Oschlies, A., Scott, V., and Vaughan, N. E.: The Effects of Carbon Dioxide Removal on the Carbon Cycle, Curr Clim Change Rep, 4, 250–265, https://doi.org/10.1007/s40641-018-0104-3, 2018b.

King, J. A., Weber, J., Lawrence, P., Roe, S., Swann, A. L. S., and Val Martin, M.: Global and regional hydrological impacts of global forest expansion, Biogeosciences, 21, 3883–3902, https://doi.org/10.5194/bg-21-3883-2024, 2024.

Koven, C. D., Arora, V. K., Cadule, P., Fisher, R. A., Jones, C. D., Lawrence, D. M., Lewis, J., Lindsay, K., Mathesius, S., Meinshausen, M., Mills, M., Nicholls, Z., Sanderson, B. M., Séférian, R., Swart, N. C., Wieder, W. R., and Zickfeld, K.: Multi-century dynamics of the climate and carbon cycle under both high and net negative emissions scenarios, Earth Syst. Dynam., 13, 885–909, https://doi.org/10.5194/esd-13-885-2022, 2022.

Kowalczyk, K. A., Amann, T., Strefler, J., Vorrath, M.-E., Hartmann, J., De Marco, S., Renforth, P., Foteinis, S., and Kriegler, E.: Marine carbon dioxide removal by alkalinization should no longer be overlooked, Environ. Res. Lett., 19, 074033, https://doi.org/10.1088/1748-9326/ad5192, 2024.

Lawrence, D. M., Hurtt, G. C., Arneth, A., Brovkin, V., Calvin, K. V., Jones, A. D., Jones, C. D., Lawrence, P. J., De Noblet-Ducoudré, N., Pongratz, J., Seneviratne, S. I., and Shevliakova, E.: The Land Use Model Intercomparison Project (LUMIP) contribution to CMIP6:rationale and experimental design, Geosci. Model Dev., 9, 2973–2998, https://doi.org/10.5194/gmd-9-2973-2016, 2016.

Li, Z., Ciais, P., Wright, J. S., Wang, Y., Liu, S., Wang, J., Li, L. Z. X., Lu, H., Huang, X., Zhu, L., Goll, D. S., and Li, W.: Increased precipitation over land due to climate feedback of large-scale bioenergy cultivation, Nat Commun, 14, 4096, https://doi.org/10.1038/s41467-023-39803-9, 2023.

Liddicoat, S. K., Wiltshire, A. J., Jones, C. D., Arora, V. K., Brovkin, V., Cadule, P., Hajima, T., Lawrence, D. M., Pongratz, J., Schwinger, J., Séférian, R., Tjiputra, J. F., and Ziehn, T.: Compatible Fossil Fuel CO2 Emissions in the CMIP6 Earth System Models' Historical and Shared Socioeconomic Pathway Experiments of the Twenty-First Century, Journal of Climate, 34, 2853–2875, https://doi.org/10.1175/JCLI-D-19-0991.1, 2021.

Loughran, T. F., Ziehn, T., Law, R., Canadell, J. G., Pongratz, J., Liddicoat, S., Hajima, T., Ito, A., Lawrence, D. M., and Arora, V. K.: Limited Mitigation Potential of Forestation Under a High Emissions Scenario: Results From Multi-Model and Single Model Ensembles, JGR Biogeosciences, 128, e2023JG007605, https://doi.org/10.1029/2023JG007605, 2023.

MacDougall, A. H., Frölicher, T. L., Jones, C. D., Rogelj, J., Matthews, H. D., Zickfeld, K., Arora, V. K., Barrett, N. J., Brovkin, V., Burger, F. A., Eby, M., Eliseev, A. V., Hajima, T., Holden, P. B., Jeltsch-Thömmes, A., Koven, C., Mengis, N., Menviel, L., Michou, M., Mokhov, I. I., Oka, A., Schwinger, J., Séférian, R., Shaffer, G., Sokolov, A., Tachiiri, K., Tjiputra, J., Wiltshire, A., and Ziehn, T.: Is there warming in the pipeline? A multi-model analysis of the Zero Emissions Commitment from CO2, Biogeosciences, 17, 2987–3016, https://doi.org/10.5194/bg-17-2987-2020, 2020.

Meinshausen, M., Nicholls, Z. R. J., Lewis, J., Gidden, M. J., Vogel, E., Freund, M., Beyerle, U., Gessner, C., Nauels, A., Bauer, N., Canadell, J. G., Daniel, J. S., John, A., Krummel, P. B., Luderer, G., Meinshausen, N., Montzka, S. A., Rayner, P. J., Reimann, S., Smith, S. J., Van Den Berg, M., Velders, G. J. M., Vollmer, M. K., and Wang, R. H. J.: The shared socio-economic pathway (SSP) greenhouse gas concentrations and their extensions to 2500, Geosci. Model Dev., 13, 3571–3605, https://doi.org/10.5194/gmd-13-3571-2020, 2020.

Meinshausen, M., Schleussner, C.-F., Beyer, K., Bodeker, G., Boucher, O., Canadell, J. G., Daniel, J. S., Diongue-Niang, A., Driouech, F., Fischer, E., Forster, P., Grose, M., Hansen, G., Hausfather, Z., Ilyina, T., Kikstra, J. S., Kimutai, J., King, A. D., Lee, J.-Y., Lennard, C., Lissner, T., Nauels, A., Peters, G. P., Pirani, A., Plattner, G.-K., Pörtner, H., Rogelj, J., Rojas, M., Roy, J., Samset, B. H., Sanderson, B. M., Séférian, R., Seneviratne, S., Smith, C. J., Szopa, S., Thomas, A., Urge-Vorsatz, D., Velders, G. J. M., Yokohata, T., Ziehn, T., and Nicholls, Z.: A perspective on the next generation of Earth system model scenarios: towards representative emission pathways (REPs), Geosci. Model Dev., 17, 4533–4559, https://doi.org/10.5194/gmd-17-4533-2024, 2024.

Melnikova, I., Boucher, O., Cadule, P., Tanaka, K., Gasser, T., Hajima, T., Quilcaille, Y., Shiogama, H., Séférian, R., Tachiiri, K., Vuichard, N., Yokohata, T., and Ciais, P.: Impact of bioenergy crop expansion on climate–carbon cycle feedbacks in overshoot scenarios, Earth Syst. Dynam., 13, 779–794, https://doi.org/10.5194/esd-13-779-2022, 2022.

Melnikova, I., Ciais, P., Tanaka, K., Vuichard, N., and Boucher, O.: Relative benefits of allocating land to bioenergy crops and forests vary by region, Commun Earth Environ, 4, 230, https://doi.org/10.1038/s43247-023-00866-7, 2023.

Merfort, L., Bauer, N., Humpenöder, F., Klein, D., Strefler, J., Popp, A., Luderer, G., and Kriegler, E.: Bioenergy-induced land-use-change emissions with sectorally fragmented policies, Nat. Clim. Chang., 13, 685–692, https://doi.org/10.1038/s41558-023-01697-2, 2023.

Merfort, L., Bauer, N., Sauer, P., Dietrich, J. P., Xiong, W., Tanaka, K., Kikstra, J. S., and Zecchetto, M.: Report on CDR portfolio climate neutrality scenarios with and without overshoot including sensitivity analysis, gridding and extensions, D1.2 of the Rescue project, Potsdam Institute for Climate Impact Research, 2025.

Moustakis, Y., Nützel, T., Wey, H.-W., Bao, W., and Pongratz, J.: Temperature overshoot responses to ambitious forestation in an Earth System Model, Nat Commun, 15, 8235, https://doi.org/10.1038/s41467-024-52508-x, 2024.

Moustakis, Y., Wey, H.-W., Nützel, T., Oschlies, A., and Pongratz, J.: No compromise in efficiency from the co-application of a marine and a terrestrial CDR method, Nat Commun, 16, 4709, https://doi.org/10.1038/s41467-025-59982-x, 2025.

O'Neill, B. C., Tebaldi, C., van Vuuren, D. P., Eyring, V., Friedlingstein, P., Hurtt, G., Knutti, R., Kriegler, E., Lamarque, J.-F., Lowe, J., Meehl, G. A., Moss, R., Riahi, K., and Sanderson, B. M.: The Scenario Model Intercomparison Project (ScenarioMIP) for CMIP6, Geosci. Model Dev., 9, 3461–3482, https://doi.org/10.5194/gmd-9-3461-2016, 2016.

Oschlies, A.: Impact of atmospheric and terrestrial CO_2 feedbacks on fertilization-induced marine carbon uptake, Biogeosciences, 6, 1603–1613, https://doi.org/10.5194/bg-6-1603-2009, 2009.

Renforth, P. and Henderson, G.: Assessing ocean alkalinity for carbon sequestration, Reviews of Geophysics, 55, 636–674, https://doi.org/10.1002/2016RG000533, 2017.

Riahi, K., Bertram, C., Huppmann, D., Rogelj, J., Bosetti, V., Cabardos, A.-M., Deppermann, A., Drouet, L., Frank, S., Fricko, O., Fujimori, S., Harmsen, M., Hasegawa, T., Krey, V., Luderer, G., Paroussos, L., Schaeffer, R., Weitzel, M., Van Der Zwaan, B., Vrontisi, Z., Longa, F. D., Després, J., Fosse, F., Fragkiadakis, K., Gusti, M., Humpenöder, F., Keramidas, K., Kishimoto, P., Kriegler, E., Meinshausen, M., Nogueira, L. P., Oshiro, K., Popp, A., Rochedo, P. R. R., Ünlü, G., Van Ruijven, B., Takakura, J., Tavoni, M., Van Vuuren, D., and Zakeri, B.: Cost and attainability of meeting stringent climate targets without overshoot, Nat. Clim. Chang., 11, 1063–1069, https://doi.org/10.1038/s41558-021-01215-2, 2021.

Sanderson, B. M., Booth, B. B. B., Dunne, J., Eyring, V., Fisher, R. A., Friedlingstein, P., Gidden, M. J., Hajima, T., Jones, C. D., Jones, C. G., King, A., Koven, C. D., Lawrence, D. M., Lowe, J., Mengis, N., Peters, G. P., Rogelj, J., Smith, C., Snyder, A. C., Simpson, I. R., Swann, A. L. S., Tebaldi, C., Ilyina, T., Schleussner, C.-F., Séférian, R., Samset, B. H., Van Vuuren, D., and Zaehle, S.: The need for carbon-emissions-driven climate projections in CMIP7, Geosci. Model Dev., 17, 8141–8172, https://doi.org/10.5194/gmd-17-8141-2024, 2024.

Schenuit, F., Böttcher, M., and Geden, O.: "Carbon Management": opportunities and risks for ambitious climate policy, SWP Comment 29/2023, Stiftung Wissenschaft und Politik, German Institute for International and Security Affairs, https://doi.org/10.18449/2023C29, 2023.

Schwinger, J., Asaadi, A., Steinert, N. J., and Lee, H.: Emit now, mitigate later? Earth system reversibility under overshoots of different magnitudes and durations, Earth Syst. Dynam., 13, 1641–1665, https://doi.org/10.5194/esd-13-1641-2022, 2022.

Schwinger, J., Bourgeois, T., and Rickels, W.: On the emission-path dependency of the efficiency of ocean alkalinity enhancement, Environ. Res. Lett., 19, 074067, https://doi.org/10.1088/1748-9326/ad5a27, 2024.

Seland, Ø., Bentsen, M., Olivié, D., Toniazzo, T., Gjermundsen, A., Graff, L. S., Debernard, J. B., Gupta, A. K., He, Y.-C., Kirkevåg, A., Schwinger, J., Tjiputra, J., Aas, K. S., Bethke, I., Fan, Y., Griesfeller, J., Grini, A., Guo, C., Ilicak, M., Karset, I. H. H., Landgren, O., Liakka, J., Moseid, K. O., Nummelin, A., Spensberger, C., Tang, H., Zhang, Z., Heinze, C., Iversen, T., and Schulz, M.: Overview of the Norwegian Earth System Model (NorESM2) and key climate response of CMIP6 DECK, historical, and scenario simulations, Geoscientific Model Development, 13, 6165–6200, https://doi.org/10.5194/gmd-13-6165-2020, 2020.

Smith, C., Ramme, L., Wells, C. D., Gjermundsen, A., Li, H., Ilyina, T., Muralidhar, A., Bourgeois, T., Schwinger, J., Romero-Prieto, A., Li, C., and Mauritzen, C.: Overshoot and (ir)reversibility to 2300 in two CO_2 -emissions driven Earth System Models, https://doi.org/10.5194/egusphere-2025-5292, 7 November 2025.

Sonntag, S., Pongratz, J., Reick, C. H., and Schmidt, H.: Reforestation in a high-CO_2 world—Higher mitigation potential than expected, lower adaptation potential than hoped for, Geophysical Research Letters, 43, 6546–6553, https://doi.org/10.1002/2016GL068824, 2016.

Sonntag, S., Ferrer González, M., Ilyina, T., Kracher, D., Nabel, J. E. M. S., Niemeier, U., Pongratz, J., Reick, C. H., and Schmidt, H.: Quantifying and Comparing Effects of Climate Engineering Methods on the Earth System, Earth's Future, 6, 149–168, https://doi.org/10.1002/2017EF000620, 2018.

Strefler, J., Bauer, N., Humpenöder, F., Klein, D., Popp, A., and Kriegler, E.: Carbon dioxide removal technologies are not born equal, Environ. Res. Lett., 16, 074021, https://doi.org/10.1088/1748-9326/ac0a11, 2021.

Strefler, J., Kowalczyk, K., Hofbauer, V., Dorndorf, T., and Baumstark, L.: Ocean liming can help achieve the Paris climate target, Environ. Res. Lett., 20, 094004, https://doi.org/10.1088/1748-9326/adf12c, 2025.

Swann, A. L. S., Fung, I. Y., and Chiang, J. C. H.: Mid-latitude afforestation shifts general circulation and tropical precipitation, Proc. Natl. Acad. Sci. U.S.A., 109, 712–716, https://doi.org/10.1073/pnas.1116706108, 2012.

Taylor, K. E., Stouffer, R. J., and Meehl, G. A.: An Overview of CMIP5 and the Experiment Design, Bulletin of the American Meteorological Society, 93, 485–498, https://doi.org/10.1175/BAMS-D-11-00094.1, 2012.

Terhaar, J.: Drivers of decadal trends in the ocean carbon sink in the past, present, and future in Earth system models, Biogeosciences, 21, 3903–3926, https://doi.org/10.5194/bg-21-3903-2024, 2024.

Tjiputra, J. F., Schwinger, J., Bentsen, M., Morée, A. L., Gao, S., Bethke, I., Heinze, C., Goris, N., Gupta, A., He, Y.-C., Olivié, D., Seland, Ø., and Schulz, M.: Ocean biogeochemistry in the Norwegian Earth System Model version 2 (NorESM2), Geosci. Model Dev., 13, 2393–2431, https://doi.org/10.5194/gmd-13-2393-2020, 2020.

Tokarska, K. B. and Zickfeld, K.: The effectiveness of net negative carbon dioxide emissions in reversing anthropogenic climate change, Environ. Res. Lett., 10, 094013, https://doi.org/10.1088/1748-9326/10/9/094013, 2015.

Tyka, M. D.: Efficiency metrics for ocean alkalinity enhancements under responsive and prescribed atmospheric p CO_2 conditions, Biogeosciences, 22, 341–353, https://doi.org/10.5194/bg-22-341-2025, 2025.

Van Vuuren, D., O'Neill, B., Tebaldi, C., Chini, L., Friedlingstein, P., Hasegawa, T., Riahi, K., Sanderson, B., Govindasamy, B., Bauer, N., Eyring, V., Fall, C., Frieler, K., Gidden, M., Gohar, L., Jones, A., King, A., Knutti, R., Kriegler, E., Lawrence, P., Lennard, C., Lowe, J., Mathison, C., Mehmood, S., Prado, L., Zhang, Q., Rose, S., Ruane, A., Schleussner, C.-F., Seferian, R., Sillmann, J., Smith, C., Sörensson, A., Panickal, S., Tachiiri, K., Vaughan, N., Vishwanathan, S., Yokohata, T., and Ziehn, T.: The Scenario Model Intercomparison Project for CMIP7 (ScenarioMIP-CMIP7), https://doi.org/10.5194/egusphere-2024-3765, 30 January 2025.

Van Vuuren, D. P., O'Neill, B. C., Tebaldi, C., Sanderson, B. M., Chini, L. P., Friedlingstein, P., Hasegawa, T., Riahi, K., Govindasamy, B., Bauer, N., Eyring, V., Fall, C. M. N., Frieler, K., Gidden, M. J., Gohar, L. K., Högner, A., Jones, A. D., Kikstra, J., King, A., Knutti, R., Kriegler, E., Lawrence, P., Lennard, C., Lowe, J., Mathison, C., Mehmood, S., Nicholls, Z., Prado, L. F., Zhang, Q., Rose, S. K., Ruane, A. C., Sandstad, M., Schleussner, C.-F., Seferian, R., Sillmann, J., Smith, C., Sörensson, A. A., Panickal, S., Tachiiri, K., Vaughan, N., Vishwanathan, S. S., Yokohata, T., Zecchetto, M., and Ziehn, T.: The Scenario Model Intercomparison Project for CMIP7 (ScenarioMIP-CMIP7), Geosci. Model Dev., 19, 2627–2656, https://doi.org/10.5194/gmd-19-2627-2026, 2026.

Wang, J., Li, W., Ciais, P., Li, L. Z. X., Chang, J., Goll, D., Gasser, T., Huang, X., Devaraju, N., and Boucher, O.: Global cooling induced by biophysical effects of bioenergy crop cultivation, Nat Commun, 12, 7255, https://doi.org/10.1038/s41467-021-27520-0, 2021.

Windisch, M. G., Humpenöder, F., Merfort, L., Bauer, N., Luderer, G., Dietrich, J. P., Heinke, J., Müller, C., Abrahao, G., Lotze-Campen, H., and Popp, A.: Hedging our bet on forest permanence for the economic viability of climate targets, Nat Commun, 16, 2460, https://doi.org/10.1038/s41467-025-57607-x, 2025.

Wu, J., Keller, D. P., and Oschlies, A.: Carbon dioxide removal via macroalgae open-ocean mariculture and sinking: an Earth system modeling study, Earth Syst. Dynam., 14, 185–221, https://doi.org/10.5194/esd-14-185-2023, 2023.

Zhou, M., Tyka, M. D., Ho, D. T., Yankovsky, E., Bachman, S., Nicholas, T., Karspeck, A. R., and Long, M. C.: Mapping the global variation in the efficiency of ocean alkalinity enhancement for carbon dioxide removal, Nat. Clim. Chang., 15, 59–65, https://doi.org/10.1038/s41558-024-02179-9, 2025.

Zickfeld, K., MacIsaac, A. J., Canadell, J. G., Fuss, S., Jackson, R. B., Jones, C. D., Lohila, A., Matthews, H. D., Peters, G. P., Rogelj, J., and Zaehle, S.: Net-zero approaches must consider Earth system impacts to achieve climate goals, Nat. Clim. Chang., 13, 1298–1305, https://doi.org/10.1038/s41558-023-01862-7, 2023.